

A THREE-DIMENSIONAL MODEL FOR SEEPAGE ANALYSIS OF CONCRETE DAMS FOUNDATIONS

J.F. Da Silva

Director of CMEC - Geotechnical Consulting Engineers. Formerly D.Sc. student at the Federal University of Minas Gerais (UFMG), Belo Horizonte, Brazil.

E.M. Da Gama

Professor of Rock Mechanics at the Department of Mining, Federal University of Minas Gerais (UFMG), Belo Horizonte, Brazil.

Abstract

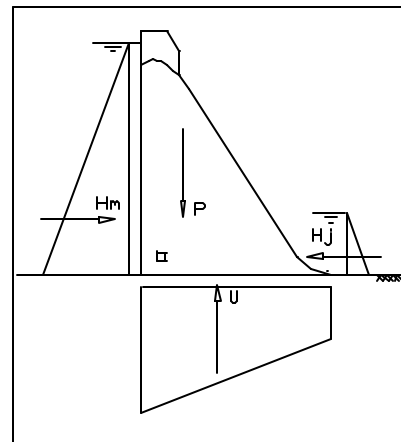
The three-dimensional flow in continuous permeable rocks under concrete dams is discussed particularly the influence of the drains in the determination of the uplift pressures needed for stability analysis. A numerical model is proposed, based on the Darcy-Weissbach law for pipes, to simulate the flow in smooth or rough drains, under laminar or turbulent regimen. Nonlinear flow in the drains is modeled by means of a “virtual drain” where Darcy’s law for smooth pipes applies. The validity of the numerical model is verified initially by comparison with the results of an analytical solution proposed by Muskat. Subsequently, the numerical model is tested by comparing its results to those of a well-documented case history, the Isamu Ikeda dam, in operation in northern Brazil. The results, in both cases, were very encouraging.

1 INTRODUCTION

Concrete dams suffer permanently the action of forces, as indicated in Figure 1. Some of these forces tend to destabilize the dam like the thrust of the upstream reservoir and the uplift pressures under its base. To counterbalance these forces there is the weight of the structure and the thrust of the downstream reservoir.

The correlation between these forces is given by the expression:

Figure 1 – Forces acting on concrete dams



$$F_s = \frac{(P - U) \tan \Phi + cA}{H_m - H_j} \quad (1)$$

where F_s is the safety factor against sliding, P is the weight of the structure (kN), H_m is the force due to the upstream reservoir (kN), H_j is the force due to the downstream reservoir (kN); U is the uplift force (kN); Φ is the friction angle along the base ($^\circ$); c is the cohesion along the base (kN/m²) and A is the area of the base (m²).

As the friction angle and the cohesion are properties of the foundation materials there are only two forces in equation (1) that can be altered by the designer and they are the weight of the structure and the uplift force.

It can also be observed in expression (1) that the safety factor is constant when the difference ($P - U$) is also constant. This means that for a required factor of safety, a small uplift force requires a small weight for the structure, in order to maintain stability.

As the weight of the structure can be altered through changes in its geometry, a method that would permit the design of an adequate subsurface drainage system to reduce the uplift pressures would lead to reductions in concrete dam costs.

In the case of earth dams the pore-pressures are estimated, with adequate precision, by means of two-dimensional flow nets, assuming the validity of Darcy's law for flow in porous materials. A flow net offers all the elements needed to estimate gradients, velocities and discharges at any point in the net.

However, tracing flow nets for concrete dams foundations would be a formidable

task since this problem is a three-dimensional one due to the presence of circular drains drilled in the rock foundation. In addition, the flow inside the drains is often nonlinear.

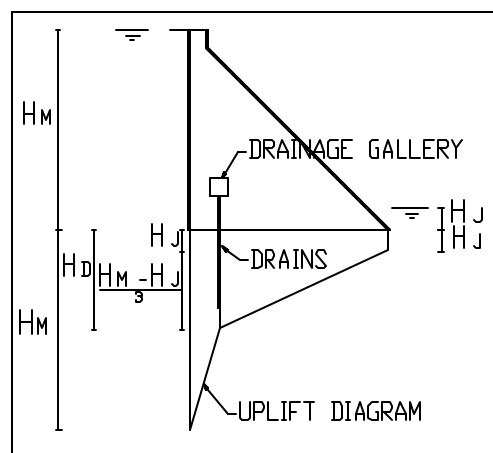
2 CURRENT PRACTICE

Designers have basically two different ways to estimate the uplift pressures under concrete dams. One is through the use of design criteria and the other by means of an analytical solution.

- design criteria

The use of design criteria is a very convenient way of estimating uplift pressures under concrete dams since they require only very simple calculations to achieve their objective. One criterion was proposed by the USBR, back in the thirties. Based on the instrumentation results of a few dams in operation, the USBR proposed⁽¹⁾ that the uplift pressures diagram be defined as indicated in Figure 2.

Figure 2 - USBR design criterion to estimate the uplift force⁽¹⁾



As shown in Figure 2, the pressure H_D acting along the line of drains was determined by the following expression:

$$H_D = H_J + \left(\frac{H_M - H_J}{3} \right) \quad (2)$$

Using the same approach the Tennessee Valley Authority (TVA), proposed a similar criterion⁽¹⁾, with the pressure acting along the line of drains given by the following expression:

$$H_D = H_J + \left(\frac{H_M - H_J}{4} \right) \quad (3)$$

It must be pointed out that these criteria do not take into account the geological conditions of the rock foundation and are used both in the case of a continuous low permeability rock or of a very fractured high permeability rock. Also, these criteria were established for particular values of drain diameter, length and spacing and for the case of one drainage gallery only.

A measure of the accuracy of these criteria is indicated in Figure 3 and Figure 4. Both the uplift pressure diagrams obtained using the TVA design criterion and those obtained from piezometer readings are shown.

Figure 3 - Uplift pressures at Hiwassee Dam⁽¹⁾

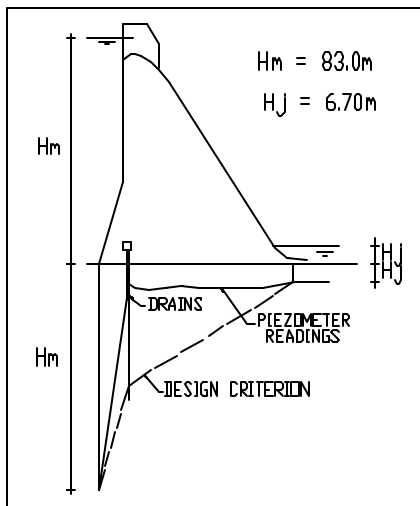


Table 1 indicates the differences between the estimated and measured uplift forces for Hiwassee and Fontana Dams. It can be seen that the differences are significant meaning that at least in these cases the design criteria used is rather conservative.

Figure 4 - Uplift pressures at Fontana Dam⁽¹⁾

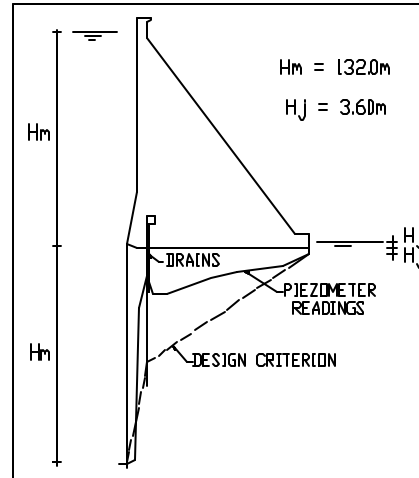


TABLE 1 - Uplift forces for Hiwassee and Fontana Dams

DAM	UPLIFT FORCES		
	Estimated (MPa/m)	Measured (MPa/m)	Differences (%)
Hiwassee	23.51	9.93	237
Fontana	51.27	28.86	178

Besides being very simple to use, one additional reason for the popularity of the design criteria is the widespread belief that they always lead to conservative estimates of the uplift forces.

However, that this is not always the case is shown in Figure 5 and Figure 6, which indicate the uplift pressures observed on some dams located in the USA. For comparison, the USBR design criterion is also shown in the figures.

Figures 5 and 6 show that for some dams the criteria is actually conservative and for others they can be considered adequate. However, the design criterion is not considered adequate for those dams whose uplift pressures fall outside the USBR diagram.

Figure 5 - Average uplift pressures in the contact dam / foundations (Apud Casagrande⁽²⁾)

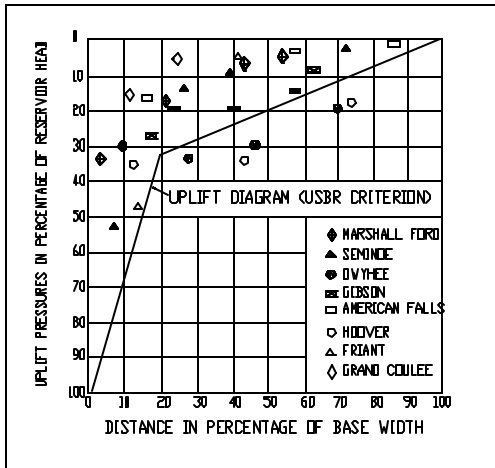
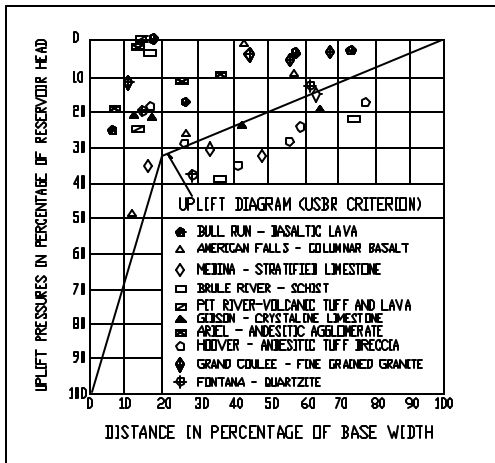


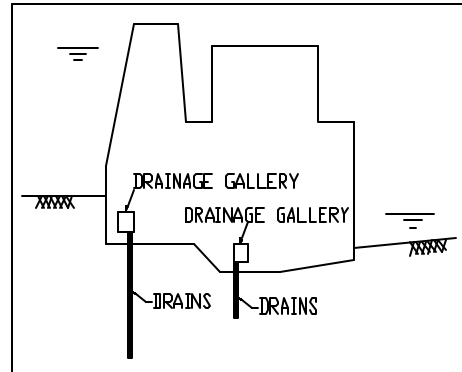
Figure 6 - Average uplift pressures in the contact dam / foundations. (Apud Serafim and Del Campo⁽³⁾)



In addition these criteria cannot be applied to structures that depart from the standard geometry shown in Figure 2.

Figure 7, which shows the combined structures of the intake and the powerhouse of a modern dam, indicates a situation that does not meet the basic conditions to be analyzed by the criteria.

Figure 7 - Combined structures of an Intake and a Powerhouse



From the discussions it is clear that the utilization of the design criteria is not an adequate way to estimate the uplift pressures under concrete dams with drains drilled in its foundations.

It should be further noticed that these criteria do not permit an estimate of the flow collected by the drains, a requirement for the design of the pumping systems of the drainage galleries.

- analytical solution

An analytical solution was developed by Muskat⁽⁴⁾ for the analysis of flow to a line of wells located between two water channels. The wells were drilled in homogeneous and isotropic materials. This solution was used by Casagrande⁽²⁾ to determine the uplift pressures acting on the base of a concrete dam with one line of smooth drains, as shown on Fig. 2.

This solution can be represented by the following expression^(2,5):

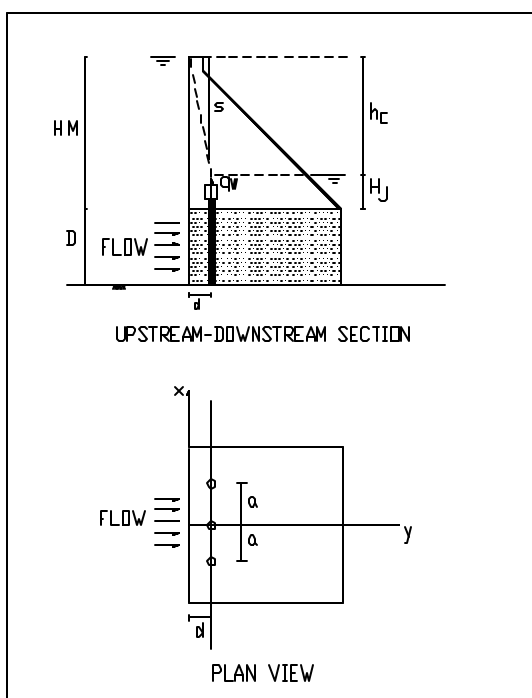
$$s(x, y) = \frac{q_w}{4p k D} \ln \frac{\cosh 2p \left(\frac{y+d}{a} \right) - \cos \frac{2p x}{a}}{\cosh 2p \left(\frac{y-d}{a} \right) - \cos \frac{2p x}{a}} \quad (4)$$

where: $q_w = k h_c a \frac{D}{d}$ (5)

and $P(x,y) = H_M - s(x,y)$ (6)

The variables present in equations (4) to (6) are indicated in Figure 8 together with the boundary conditions of the problem.

Figure 8 - Symbols and boundary conditions for determination of uplift pressures



The meaning of the variables is the following: $S(x,y)$ is the z-ordinate (m) of a point of coordinates (x,y) , on the base of the dam, q_w is the flow in the drain (m^3/s), a is the drain spacing (m), d is the distance between the upstream face and the line of drains (m), D is the thickness of the foundation(m), h_c is the total head (m), $P(x,y)$ is the uplift pressure of a point of coordinates (x,y) , on the base of the

dam and H_M is the depth of the upstream reservoir (m).

Expression(4) is based on the following assumptions:

- the flow is permanent and the water is incompressible;
- the foundation material is homogeneous, isotropic, saturated and incompressible;
- the drains are smooth with length equal to the total thickness of the foundation;
- the flow is laminar e occurs only from the upstream side along a vertical face in the foundations;
- there is no flow downstream of the line of drains;
- the dam base is horizontal.

Taking equation (5) into (4), one has:

$$s(x, y) = \frac{h_c a}{4p d} \ln \frac{\cosh 2p \left(\frac{y+d}{a} \right) - \cos \frac{2p x}{a}}{\cosh 2p \left(\frac{y-d}{a} \right) - \cos \frac{2p x}{a}} \quad (7)$$

Equation (7) states that the uplift pressures are independent of the rock permeability, the drains diameter and the thickness of the foundation.

Due to the limitations discussed above, a structure such as the one depicted in Figure 7 cannot be analyzed by means of equation (7). Besides its geometry being very different from that assumed in the development of the equation, the foundation materials of real dams are seldom homogeneous or isotropic.

Despite these limitations the analytical solution is an excellent tool for the assessment of the accuracy of numerical methods eventually developed to solve this problem.

3 FLOW IN CONTINUOUS ROCK MASSES AND IN DRAINS

As pointed out the design criteria are not applicable to all situations and do not take into account the geological conditions of the foundation materials. Also they are overly conservative in some cases and too liberal in others. The analytical solution, due to its inherent limitations is seldom used in design.

The ideal solution to this problem should be similar to the one used in the design of earth dams where the values of pore-pressures, gradients, velocities and quantities of seepage can be obtained at any point of the flow nets. Also, the flow nets are traced taking into account both the embankment and foundation materials' geotechnical properties and the geometry of the structure.

In concrete dams flow occurs through the rock foundation into the drains and to the drainage galleries. Therefore to obtain the distribution of pore-pressures, gradients, velocities and discharges one must take into account the geotechnical properties of the foundation materials, the structure's geometry and the characteristics of the subsurface drainage system comprised by the drains and the drainage galleries.

To this effect, a discussion of the laws that represent the flow in continuous permeable rock masses and the flow in circular drains follows.

3.1 Flow in Continuous Permeable Rock Masses

The permanent flow in continuous permeable rock masses, saturated and incompressible, is represented by Darcy's law for porous media.

Darcy's law can be represented by the following expression:

$$V = k i \quad (8)$$

where V is the flow velocity (m/s), k is the coefficient of permeability (m/s) and i is the hydraulic gradient.

3.2 Flow Regimen in Circular Drains

The following non-dimensional relationship is denominated Reynolds' number:

$$N_R = \frac{VD}{\mathbf{n}} \quad (9)$$

where N_R is Reynolds' number, V is the flow velocity in the drain (m/s), D is the drain diameter (m) and \mathbf{n} is the kinematic viscosity (m^2/s)

The kinematic viscosity (\mathbf{n}), is given by Poiseuille's formula⁽⁶⁾:

$$\mathbf{n} = \frac{1.78 \times 10^{-6}}{1 + 0.0337t + 0.000221 t^2} \quad (10)$$

where "t" is the water temperature in degrees Celsius.

When Reynolds' number is smaller than 2100 ($N_R < 2100$) the flow in the drain occurs in linear or laminar regime. When N_R é larger than 3000 the flow is turbulent.

When N_R is between 2100 e 3000, a transition regime, the flow oscillates between laminar and turbulent.

3.2.1 Linear (laminar) flow in drains

The expression that represents the linear flow in drains is Darcy's law for smooth pipes under laminar regime:

$$V_{\text{drain}} = \frac{g D^2}{32n} i \quad \text{or} \quad V_{\text{drain}} = "K_{\text{drain}}" i \quad (11)$$

where V_{drain} is the flow velocity in the drain (m/s), g is gravitational acceleration (m/s^2), " K_{drain} " is the coefficient of permeability of the smooth drain "equivalent" to the K coefficient (expression 8) and equal to:

$$K_{\text{drain}} = \frac{g D^2}{32n} \quad (12)$$

3.2.2 Nonlinear flow in drains

The nonlinear flow in either smooth or rough drains, under laminar or turbulent flow, can be represented by Darcy-Weisbach equation⁽⁶⁾ for pipes:

$$h_f = f \frac{L V^2}{D 2g} \quad \text{or} \quad v = \sqrt{\frac{2gDi}{f}} \quad (13)$$

where h_f is the energy loss (m), f is the roughness coefficient and L is the drain's length (m).

The roughness coefficient "f", both for smooth or rough drains, is a function of the flow regime.

3.2.3 Determination of "f" for laminar flow

The coefficient "f", for smooth or rough

drains, is calculated by the expression:

$$f = \frac{64}{N_R} \quad (14)$$

Taking equation (14) into equation (13) Darcy's equation for pipes (11) is again obtained.

This indicates that, under a laminar regime, the flow, both by Darcy's or Darcy-Weissbach's equation, is independent of drain roughness.

3.2.4 Determination of "f" for turbulent flow

a)- Rough drains

The determination of "f" for rough drains both under transition or turbulent regimen ($N_R > 2100$), is performed by means of Colebrook's formula⁽⁶⁾:

$$\frac{1}{\sqrt{f}} = -2 \log \left(\frac{\frac{h_a}{D}}{3.71} + \frac{2.51}{N_R \sqrt{f}} \right) \quad (15)$$

where h_a is the magnitude of the drain wall roughness (m)

The relation

$$rr = \left(\frac{h_a}{D} \right) \quad (16)$$

is known as relative roughness.

Due to the difficulties in calculating "f" because it appears on both sides of equation (15), Moody⁽⁶⁾ suggested an expression for a first estimate of its value:

$$f = 0.0055 \left[1 + \left(20000 \frac{h_a}{D} + \frac{10^6}{N_R} \right)^{\frac{1}{3}} \right] \quad (17)$$

The value of "f", estimated through expression (17), is more or less 5% of the value given by expression (15)⁽⁶⁾.

b) - Hydraulically smooth drain

The limit layer thickness "δ" for circular drains is given by the expression:

$$d = \frac{32.8D}{N_R \sqrt{f}} \quad (18)$$

When the magnitude of the drain wall roughness (h_a) satisfies the relation $h_a < \frac{d}{3}$, it is said that flow occurs in a hydraulically smooth drain. In this case "f" is calculated by an expression suggested by Nikuradse⁽⁶⁾:

$$f = 0.0032 + 0.221 (N_R)^{-0.237} \quad (19)$$

3.2.5 Velocity and discharge

The discharge in drains, regardless of the flow regime, is equal to:

$$Q_{\text{Drain}} = V_{\text{Drain}} A \quad (20)$$

where A is the cross-sectional area of the drain, calculated by the expression:

$$A = \frac{\pi D^2}{4} \quad (21)$$

and V_{Drain} is given by the equation:

$$V_{\text{Drain}} = \sqrt{\frac{2gDi}{f}} \quad (22)$$

Therefore, the discharge in the drain is equal to:

$$Q_{\text{Drain}} = \sqrt{\frac{2gDi}{f}} \cdot \frac{\pi D^2}{4} \quad (23)$$

4 FLOW IN CONCRETE DAMS FOUNDATIONS

Based on Darcy's law that represents the flow in continuous permeable rocks and in Darcy-Weissbach's equation for circular drains, a numerical model was developed, through the finite element method, to analyze the tri-dimensional flow of water under concrete dams.

A computer code (DW3D) was developed for the analysis of tri-dimensional flow of water in permeable continuous rocks. Subsequently, a subroutine was incorporated for the analysis of linear flow in smooth drains. Finally a model for the analysis of nonlinear flow for both smooth and rough drains was incorporated into the code.

4.1 Tri-dimensional flow in permeable continuous rocks

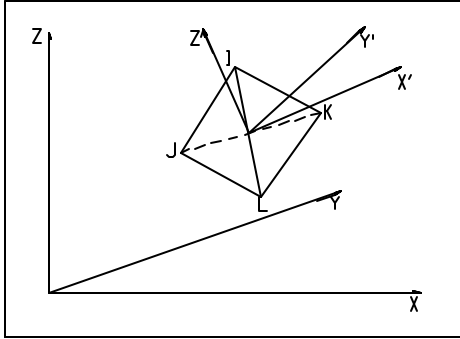
In continuous permeable rocks seepage occurs through the rock matrix. To incorporate this flow into the analysis two types of three-dimensional finite elements were used: a regular prism with eight nodes and a triangular prism with six nodes. Each prism was then adequately subdivided into tetrahedrons. Therefore only the stiffness matrix for a tetrahedron needed to be developed.

4.1.1 Flow in the tetrahedron

Figure 9 shows a tetrahedron limited by nodal points I, J, K e L. Assuming that the permeability tensor is symmetric it is

possible to define a X' , Y' e Z' system of local coordinates, called principal system, where the permeability tensor is diagonal and the crossed permeabilities are equal to zero. Figure 9 also shows a XYZ system of global coordinates.

Figure 9 - A tetrahedron finite element with flow in X' , Y' and Z' directions



It was admitted that the flow could be represented by Darcy's law for porous materials which, in three dimensions, has the following expressions:

$$\begin{aligned} V_{x'} &= k_{x'} i_{x'} \\ V_{y'} &= k_{y'} i_{y'} \\ V_{z'} &= k_{z'} i_{z'} \end{aligned} \quad (24)$$

where $V_{x'}$ is the flow velocity (m/s), $K_{x'}$ is the coefficient of permeability (m/s) and $i_{x'}$ is the hydraulic gradient, all in direction X' . Similar expressions can be written for axes Y' and Z' .

Expressions (24) can be represented using Hubbert's approach⁽⁷⁾:

$$\begin{aligned} V_{x'} &= -K_{x'} \left(\frac{\partial P}{\partial x'} + \mathbf{r} g_{x'} \right) \\ V_{y'} &= -K_{y'} \left(\frac{\partial P}{\partial y'} + \mathbf{r} g_{y'} \right) \end{aligned} \quad (25)$$

$$V_{z'} = -K_{z'} \left(\frac{\partial P}{\partial z'} + \mathbf{r} g_{z'} \right)$$

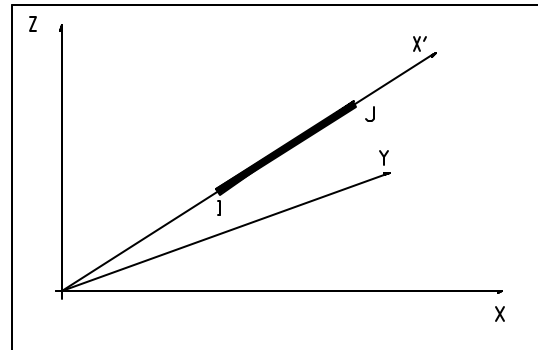
where P is the pressure at a point inside the element (kN/m^2), ρ is the water density (kN/m^3).

Details of the derivation of the stiffness matrix for the tetrahedron are presented elsewhere⁽⁸⁾.

4.1.2 Linear flow inside the drain element

Figure 10 shows a one-dimensional finite element with nodal points I and J representing a smooth drain with water flowing in the principal direction X' . It also shows a global coordinate system XYZ .

Figure 10 – A one-dimensional finite element IJ representing a drain



Assuming that the laminar flow in the drain can be represented by Darcy's law for smooth pipes (11), one has:

$$V_{\text{drain}} = \frac{g D^2}{32\mathbf{n}} i \quad (11)$$

This equation can be expressed in the following form:

$$V_{x'} = K_{x'} i_{x'} \quad (26)$$

Equation (26) can be represented using Hubbert's approach⁽⁷⁾:

$$V_{x'} = -K_{x'} \left(\frac{\partial P}{\partial x'} + \mathbf{r} g_{x'} \right) \quad (27)$$

In matrix form, the flow velocity in the drain is given by the expression:

$$\{V_{x'}\} = -[K_{x'}] \frac{1}{x'_j - x'_i} [-1 \ 1] \begin{Bmatrix} P_i \\ P_j \end{Bmatrix} - [K_{x'}] \{ \mathbf{r} g_{x'} \} \quad (28)$$

The flow quantities in the nodes are:

$$\begin{Bmatrix} Q_i \\ Q_j \end{Bmatrix} = \begin{bmatrix} \frac{A k_{x'}}{L} & -\frac{A k_{x'}}{L} \\ -\frac{A k_{x'}}{L} & \frac{A k_{x'}}{L} \end{bmatrix} \begin{Bmatrix} P_i \\ P_j \end{Bmatrix} + \begin{Bmatrix} A k_{x'} \mathbf{r} g \sin \Theta \\ -A k_{x'} \mathbf{r} g \sin \Theta \end{Bmatrix} \quad (29)$$

where Q_i is the flow quantity at node i (m^3/s), Q_j is the flow quantity at node j (m^3/s), P_i is the pressure at nodal point i (kN/m^2), P_j is the pressure at nodal point j (kN/m^2), Θ is the angle between axes X e X' ($^\circ$), A is the cross-sectional area (m^2) and L is the length of the drain (m).

In expression (29), matrix:

$$\{K\} = \begin{bmatrix} \frac{A k_{x'}}{L} & -\frac{A k_{x'}}{L} \\ -\frac{A k_{x'}}{L} & \frac{A k_{x'}}{L} \end{bmatrix} \quad (30)$$

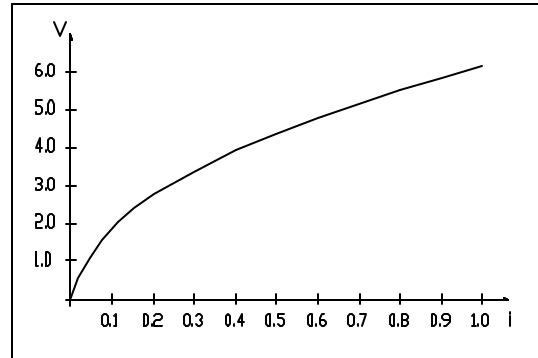
is the stiffness matrix for the drain element.

4.1.3 Nonlinear flow in drains

As pointed out, the general equation for water flow in smooth or rough drains (13), under laminar or turbulent flow, is nonlinear, as shown on Figure 11 which represents the variation of velocities in a

real drain as a function of hydraulic gradients.

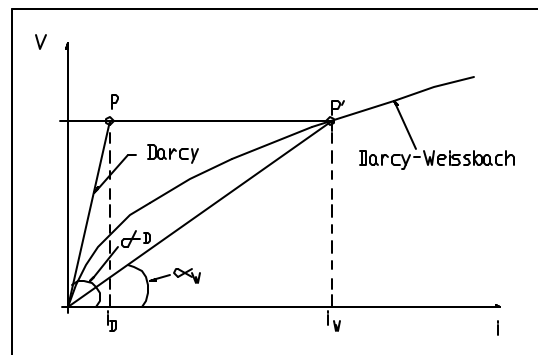
Figure 11 – Velocity versus hydraulic gradients (Darcy-Weissbach)



To take into account the non-linearity of equation (13), by means of the finite element method, it was necessary to develop a model to simulate nonlinear flow in drains through linear increments of flows. This was accomplished in the following manner:

In Figure 12, the line with inclination (α_D) represents the linear flow (Darcy) in a smooth "virtual drain" having at the outset a diameter equal to the diameter of the rough real drain (Darcy-Weissbach).

Figure 12 – Iterative Method to obtain the nonlinear behavior of real drains



Initially the velocities are the same for both drains, as indicated by points P and P' on Figure 12, but the gradients are different since the "equivalent coefficient of permeability" (12) of the drains are, respectively :

$$K_D = \tan(\alpha_D) \text{ (virtual)} \quad (31)$$

$$K_W = \tan(\alpha_W) \text{ (real)}$$

However, accordingly to expression (12), increasing or decreasing the virtual drain diameter will cause a correspondent increase or decrease in the value of its equivalent permeability (K_D). Therefore, through adequate changes in the virtual drain diameter it is always possible to make (α_D) to approach (α_W).

When convergence is achieved, the flow in both drains will be the same and although they have different diameters at this point, there will be total correspondence of velocities, gradients and discharge between the virtual and the real drain. This process is repeated, by successive iterations, for each and every finite element that comprises the drain.

Convergence is achieved when:

$$\frac{i_D - i_W}{i_W} \leq tol \quad (32)$$

where i_D is the gradient in the virtual drain, i_W is the gradient in the real drain and tol is the admitted tolerance.

5 ASSESMENT OF THE MODEL

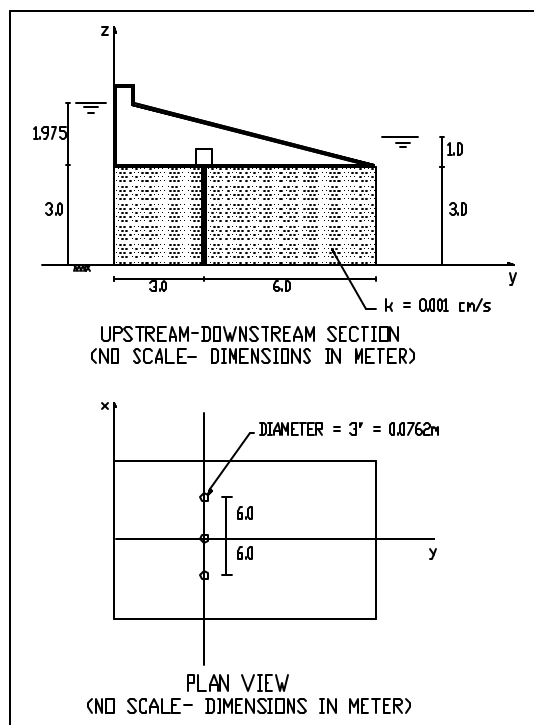
5.1 Linear flow – Isotropic media

To assess the accuracy of the proposed model a comparison was made with the

results obtained through the analytical solution (4).

The example used is indicated in Figure 13. The results obtained by both the model and the analytical solution are shown in Figures 14 e 15 which depicts the uplift pressure diagrams both in the upstream-downstream and in the drain to drain sections. Both diagrams were drawn on sections passing through the drains.

Figure 13 – Example for determination of uplift pressures on a concrete dam



It can be seen that the uplift diagrams obtained by both methods are very close.

The discharges in the drains calculated using the analytical solution and the proposed numerical method were respectively $5.9 \times 10^{-5} \text{ m}^3/\text{s}$ and $6.5 \times 10^{-5} \text{ m}^3/\text{s}$.

Figure 14 – Uplift pressures diagram - Upstream-downstream section

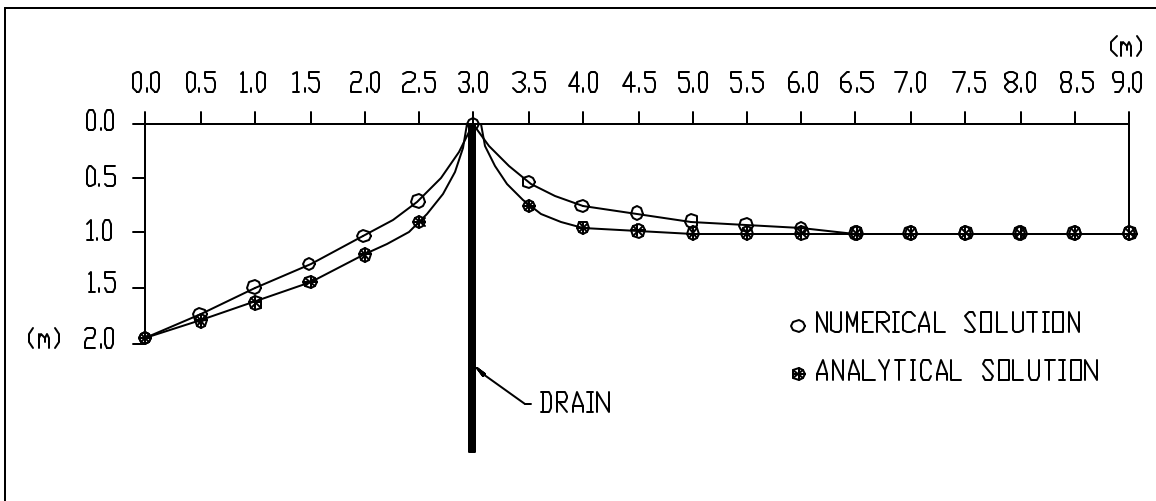
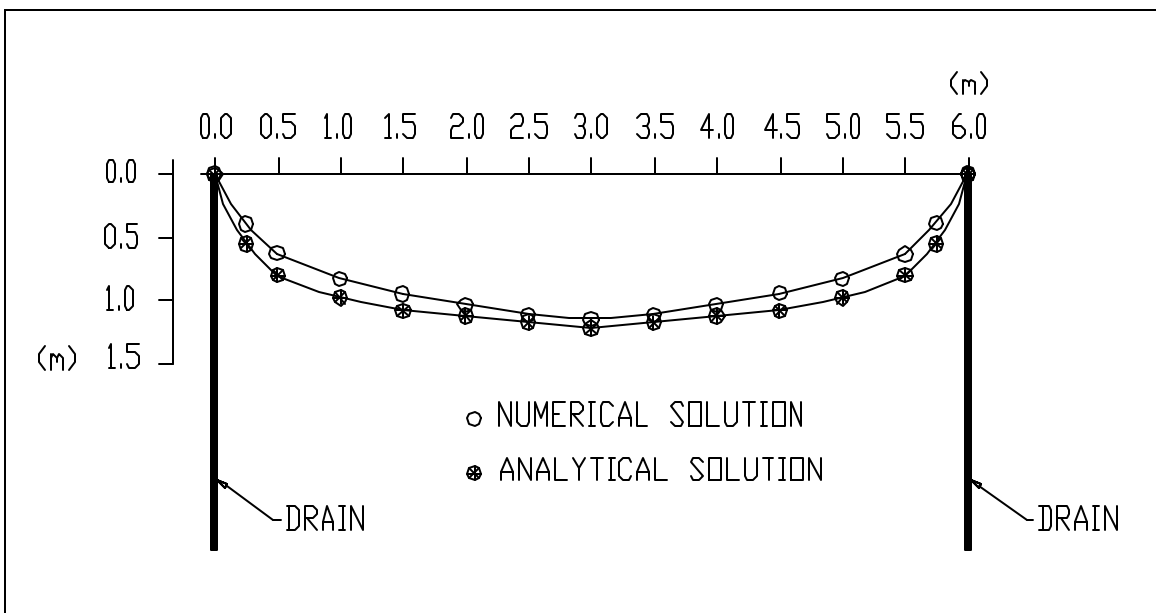


Figure 15 - Uplift pressures diagram - Drain to drain section



5.2 Nonlinear flow - Non isotropic media - Case history

5.2.1 Isamu Ikeda Dam

It has been demonstrated that the proposed model is adequate for the analysis

of flow under concrete dams when the foundation materials are homogeneous and isotropic and the flow in the drains is linear. These conditions however are seldom met with in practice and the adequacy of the model must therefore be checked against a real case.

Hence, the results of a flow analysis performed for a well-instrumented dam, using the proposed model, is presented.

The Isamu Ikeda dam is situated on Balsas river, in northern Brazil, and belongs to CELTINS – Companhia de Energia Elétrica do Estado do Tocantins.

Figure 16 shows a cross-section through the structures of block number 2, one of the four blocks that comprises the intake and powerhouse complex. This block has been chosen because it contains the piezometers installed in the dam foundations.

Figure 16 – Cross-section through the intake and powerhouse

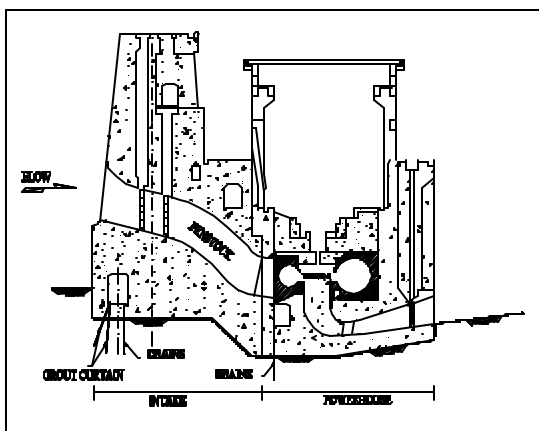


Figure 17 shows the dam geometry and the relevant geological and geotechnical conditions of the foundation⁽⁹⁾. Figure 18 was drawn along the same section and shows the drainage system geometry and the location of the piezometers⁽⁹⁾.

5.2.2 Basic data

– drains geometry

The basic data regarding the drains geometry are:

- diameter = 76mm (3")
- spacing, upstream gallery = 3.0m
- length, upstream gallery = 16.0m
- spacing, downstream gallery = 4.5m
- length, downstream gallery = 7.5m
- . magnitude of the drain wall roughness = 0.001m a 0.005m (1 to 5mm)

– piezometric data

The piezometer readings used in this paper were extracted from a designer's report⁽⁹⁾ which contain data ranging from May 1983 to August 1984. These data are indicated in Figure 19. The upstream and downstream reservoir levels are indicated in Figure 20.

The data set used in the analysis and shown in Table 2, spans from August 1983 to June 1984, because they present almost constant values in this range.

Table 2 – Piezometers readings

Piezometer	Pressure head (m)
PZ1	9.0
PZ2	3.4
PZ3	11.0
PZ4	9.0 to 9.3
PZ5	8.1
PZ6	4.7
PZ7	7.3 to 8.3
PZ8	10.0
PZ1*	6.0
PZ2*	3.2

- reservoir levels:

- . upstream = 266.58 m
- . downstream = 249.0 m

Figure 17 – Cross-section along block 2

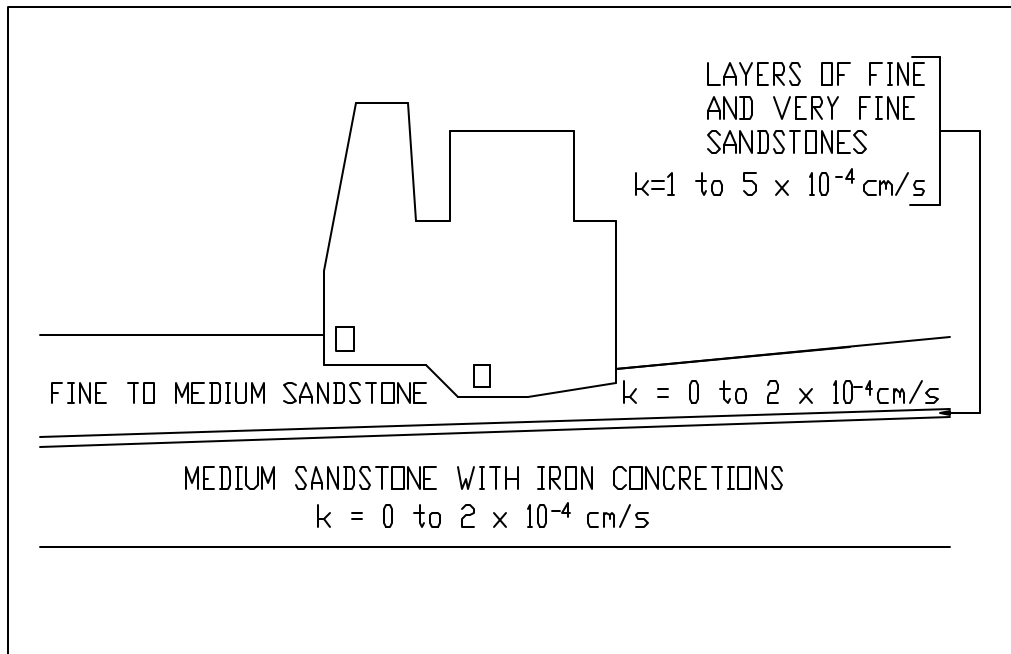


Figure 18 – Foundation drainage system and piezometers

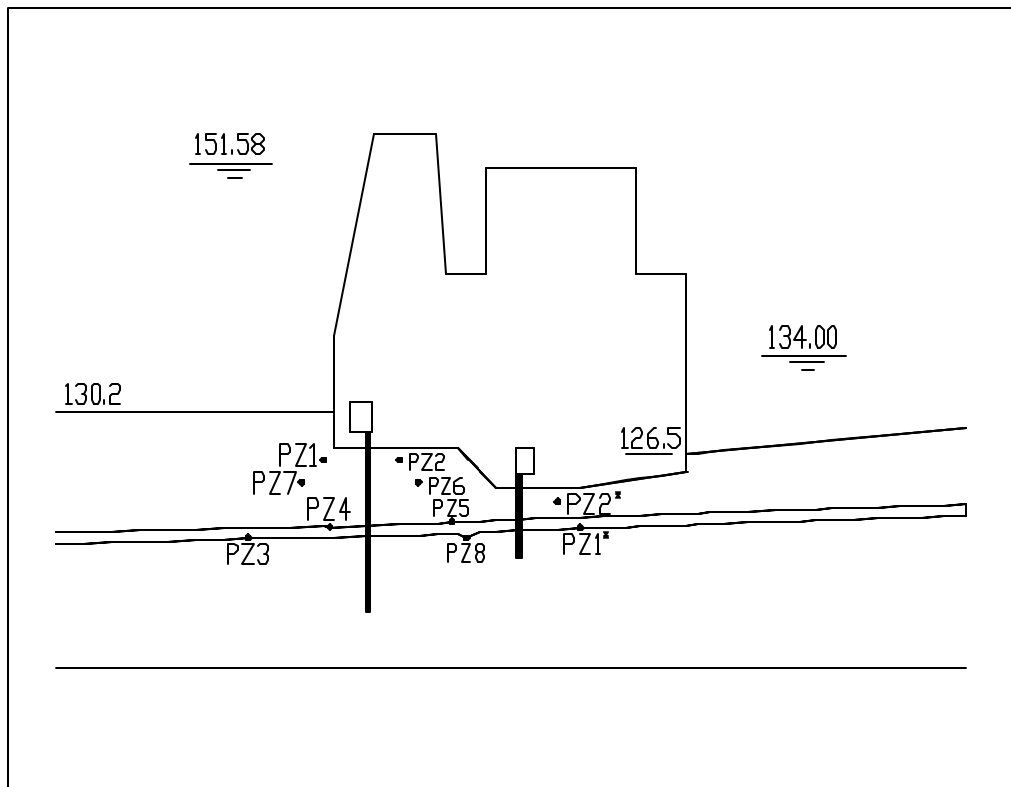


Figure 19 – Piezometric readings

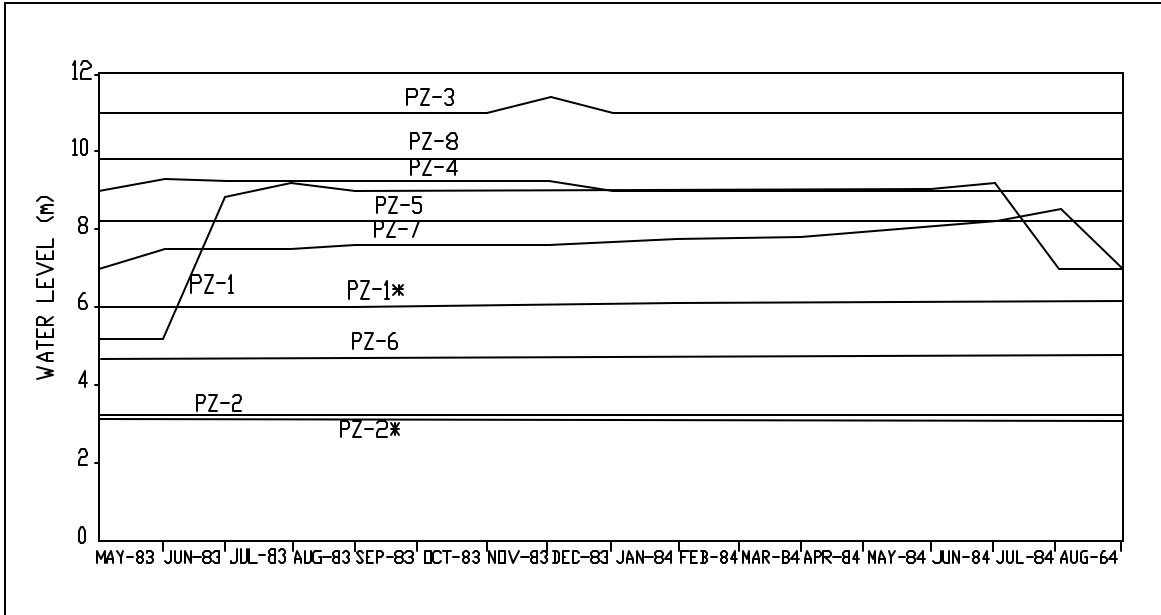
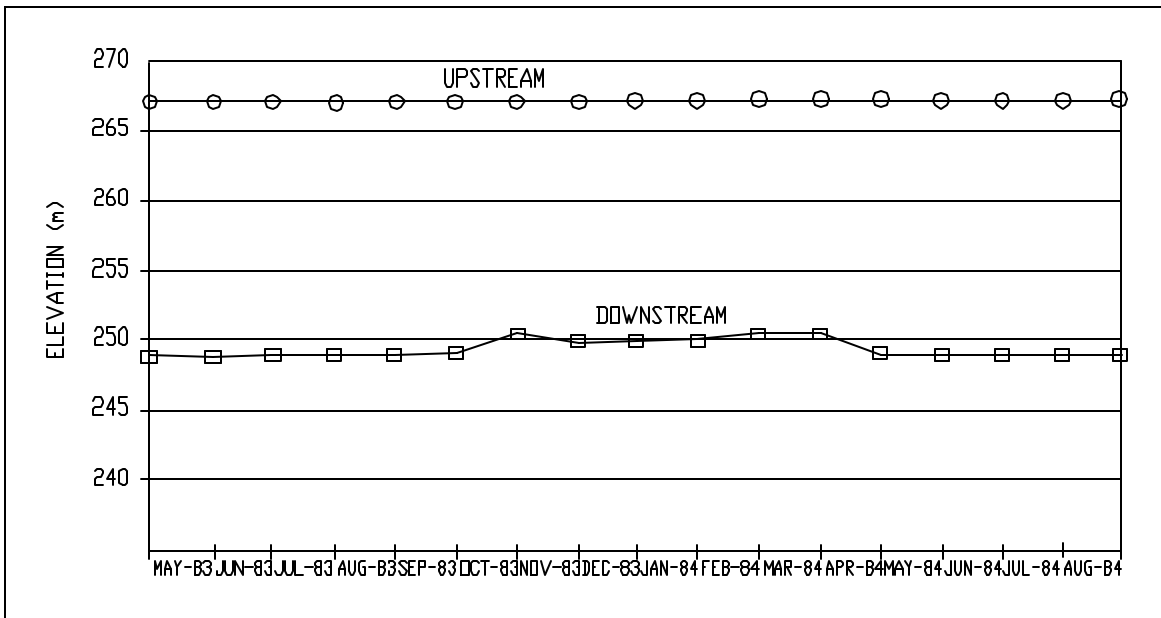


Figure 20 – Upstream and downstream reservoir levels



In the system of coordinates used in this paper (Figure 18) these levels correspond to 151.58 and 134.0, respectively.

$$\text{Angle } (x',y) = \text{Angle } (y',x) = 90^{\circ}$$

$$\text{Angle } (x',z) = \text{Angle } (z',x) = 88.5^{\circ}$$

$$\text{Angle } (y',z) = \text{Angle } (z',y) = 90^{\circ}$$

– permeability data

The available data related to the permeability of the foundation materials were obtained by means of water pressure tests (Lugeon) which presented the following values:

. fine to medium sandstone:

$$k_{x'} = 2 \times 10^{-4} \text{ cm/s}$$

. layers of fine and very fine sandstones:

$$k_{x'} = 2 \times 10^{-4} \text{ cm/s}$$

. medium sandstone with iron concretions: $k_{x'} = 2 \times 10^{-4} \text{ cm/s}$

These values, obtained in tests in vertical holes, correspond roughly to the horizontal coefficients of permeability.

However, as indicated in expression (24), the analysis of a tri-dimensional flow requires the full knowledge of the permeability tensor. Therefore, the missing coefficients of permeability had to be estimated, as discussed later on. The angles that the principal directions of the permeabilities ($x'y'z'$) make with the global coordinate system (xyz) (Figure 9), are also unknown and were inferred assuming first that the direction of $k_{x'}$ was sub-horizontal and parallel to the direction of the sandstone layers. The directions of $k_{y'}$ and $k_{z'}$ were assumed as normal to $k_{x'}$ and the resultant angles were:

$$\text{Angle } (x',x) = 1.5^{\circ}$$

$$\text{Angle } (y',y) = 0^{\circ}$$

$$\text{Angle } (z',z) = 1.5^{\circ}$$

– finite element mesh

An upstream-downstream section showing the finite element mesh used in the analysis is shown in Figure 21.

5.2.3 – Flow Analysis

a) isotropic materials

Initially, since only one of the coefficients of permeability was known, it was assumed that the foundation materials were isotropic with the following values for the coefficients of permeability:

. fine to medium sandstone:

$$k_{x'} = k_{y'} = k_{z'} = 2 \times 10^{-4} \text{ cm/s}$$

. layers of fine and very fine sandstones:

$$k_{x'} = k_{y'} = k_{z'} = 2 \times 10^{-4} \text{ cm/s}$$

. medium sandstone with iron concretions: $k_{x'} = k_{y'} = k_{z'} = 2 \times 10^{-4} \text{ cm/s}$

In addition it was assumed the existence of a higher permeability layer, 1.0m thick, along the base of the dam, comprised of sandstone shattered by blasting. The coefficients of permeability for this layer were assumed as:

$$k_{x'} = k_{y'} = k_{z'} = 2 \times 10^{-3} \text{ cm/s}$$

The analysis results are indicated in Table 3. It can be seen that the results are very different from the observed values, showing that the assumption of isotropy was not a valid one. This result was somehow expected, since sandstones generally are non-isotropic materials.

Figure 21 – Finite element mesh - Upstream-downstream section

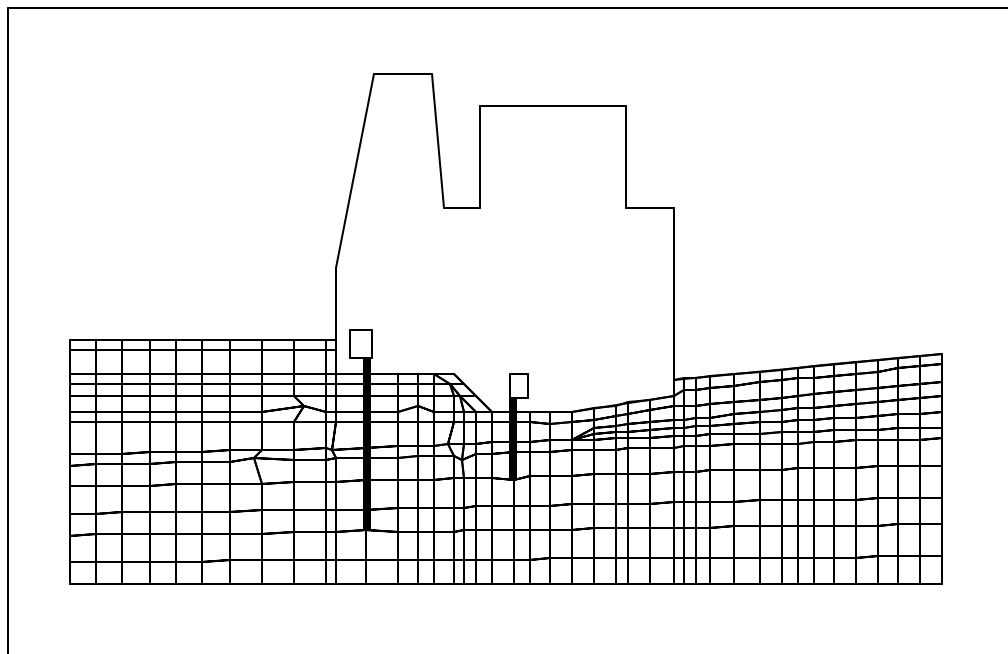


Table 3 – Observed and Calculated Pressures - Isotropic Materials

Piezometer	Observed pressure head (m)	Calculated pressure head (m)
PZ1	9.0	14.9
PZ2	3.4	2.7
PZ3	11.0	22.2
PZ4	9.0 to 9.3	14.3
PZ5	8.1	6.9
PZ6	4.7	4.1
PZ7	7.3 to 8.3	16.8
PZ8	10.0	8.2
PZ1*	6.0	8.3
PZ2*	3.2	4.9

b) materials with sub-vertical anisotropy

Since there was no available data a trial and error procedure was implemented to determine values for the coefficients of permeability that could represent adequately the anisotropy of the foundation materials.

At the same time the analysis using these values should result in values for the pressures near those indicated by the piezometer readings.

The trial and error procedure indicated the following values for the coefficients of permeability:

. fine to medium sandstone:
 $k_x' = k_y' = 1.8 \times 10^{-4}$
 and $k_z' = 2.1 \times 10^{-5}$ cm/s

. layers of fine and very fine sandstones:
 $k_x' = k_y' = 1.8 \times 10^{-4}$
 and $k_z' = 2.1 \times 10^{-5}$ cm/s

. medium sandstone with iron concretions:

$$k_x' = k_y' = 1.8 \times 10^{-4} \text{ cm/s}$$

$$\text{and } k_z' = 2.1 \times 10^{-5} \text{ cm/s}$$

. layer shattered by blasting:

$$k_x' = k_y' = 1.8 \times 10^{-3}$$

$$\text{and } k_z' = 6 \times 10^{-4} \text{ cm/s}$$

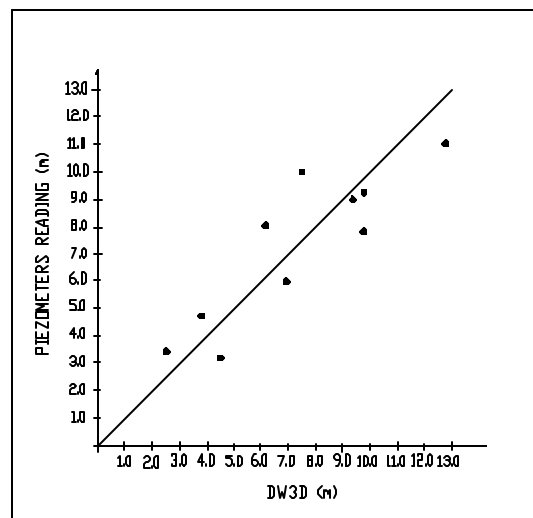
These values indicate a sub-vertical (Z) anisotropy of the order of 8.5 for the sandstones and 3 for the layer shattered by blasting. The value of 8.5 for the sandstones appears reasonable since sedimentary materials could present even higher degrees of anisotropy. As for the shattered layer, a value of 3 can also be considered reasonable since blasting has a the tendency to reduce the degree of anisotropy.

The results of the non-isotropic analysis with the permeability values discussed above are shown on Table 4 and on Figure 22.

Table 4 – Observed and calculated pore-pressures - Non-isotropic materials

Piezometer	Observed pressure head (m)	Calculated pressure head (m)
PZ1	9.0	9.3
PZ2	3.4	2.5
PZ3	11.0	12.7
PZ4	9.0 to 9.3	9.9
PZ5	8.1	6.2
PZ6	4.7	3.7
PZ7	7.3 to 8.3	9.7
PZ8	10.0	7.5
PZ1*	6.0	7.0
PZ2*	3.2	4.5

Figure 22 - Observed and calculated pore-pressures - Non-isotropic materials



Despite the limitations imposed by the assumptions regarding the permeability tensor, the pore-pressures results of the non-isotropic analysis are close to the values indicated by the piezometer readings.

The results indicate the importance of obtaining the permeability tensor for the foundation materials and field tests have been developed for this purpose. Because this topic is beyond the scope of this paper, the interested reader is referred to the literature on the subject⁽¹⁰⁾.

5.2.4 – Determination of the discharges

Table 5 presents the ranges of discharges measured in the drains of both the upstream and downstream drainage galleries, together with the values determined in the non-isotropic analysis. Although there is a somewhat larger variation for the discharges measured on the drains of the downstream gallery, the agreement between measured and calculated values are reasonably good.

Table 5 – Measured and calculated discharges in the drains

Gallery	Measured Discharges (l/min)	Calculated Discharges (l/min)
Upstream	7.5 to 9.2	8.5
Downstream	1.5 to 7.1	6.1

Figure 23 shows the uplift diagrams obtained through the non-isotropic flow analysis for upstream-downstream sections along an upstream and a downstream drain, respectively. It is also shown, for comparison, the uplift diagrams used in the original design and based on expression (2).

Figure 24 shows the correspondent uplift diagrams for flank to flank sections along the upstream and downstream lines of drains, respectively.

5.3 – Flow into the drains

Table 6 indicates the gradients, velocities and Reynolds numbers along a typical drain from its bottom up the floor of the upstream drainage gallery. One interesting point is that the flow is laminar along the bottom and middle sections of the drain, becoming turbulent only in the vicinity of the gallery floor.

6 CONCLUSIONS

Nonlinear flow in drains drilled in the rock foundations of concrete dams, represented by Darcy-Weissbach law, can be modeled through the finite element method using the concept of “virtual drain”.

The model allows the determination of pressures, gradients, velocities and discharges at any point in the foundations of concrete dams taking into account the influence of smooth or rough drains subjected to laminar or turbulent flow.

A comparison of the model results with those of an analytical solution has shown good agreement. Since the model was developed through the finite element method it does not suffer from the limitations of the analytical solution. Therefore, it can be applied to the analysis of water flow under concrete dams supported by continuous isotropic or non-isotropic, homogeneous and non-homogeneous rocks regardless of the geometries of the dam and drainage systems.

The analysis performed for a well-documented case history has shown good agreement between the observed and the calculated values of pressures and discharges, despite the assumptions regarding the foundation materials permeability tensors.

It is concluded that the proposed model is adequate for the determination of the uplift pressures necessary for concrete dams stability analysis and of the discharges needed for the design of the drainage galleries pumping systems provided there is an adequate knowledge of the permeability tensors for the foundation materials.

7 REFERENCES

- 1 - Davis, C. V., "Concrete dams, basic principles of design", In: "Handbook of applied hydraulics", Edited by Davis, C.V. e Sorensen, K.E., Third Edition, McGraw-Hill, 1969, Section 9, p.9-1 to 9-34.

Figure 23 - Uplift diagrams for upstream-downstream sections

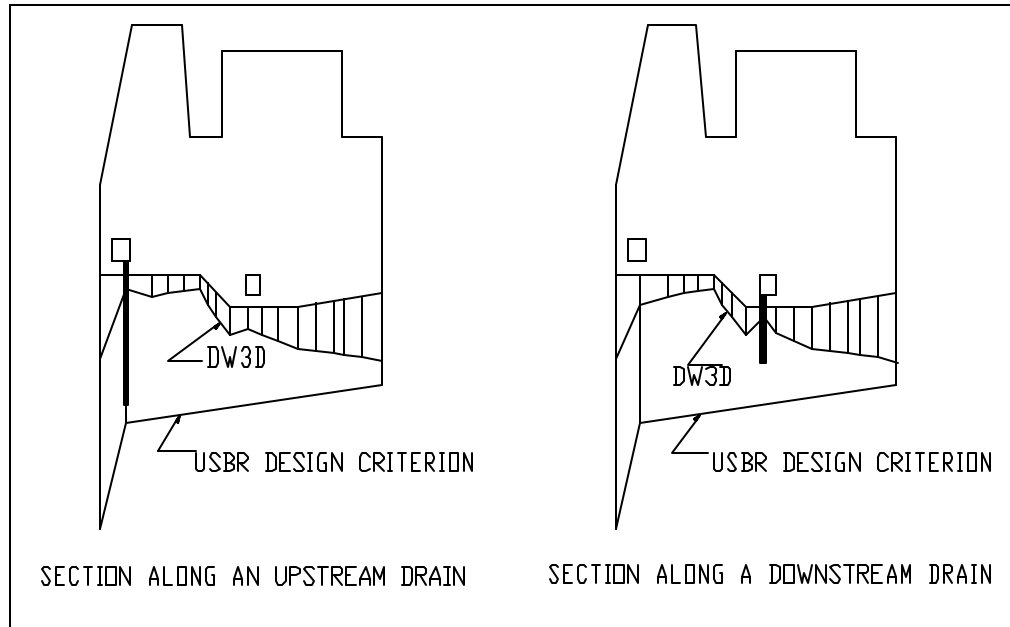


Figure 24 - Uplift diagrams for flank to flank sections

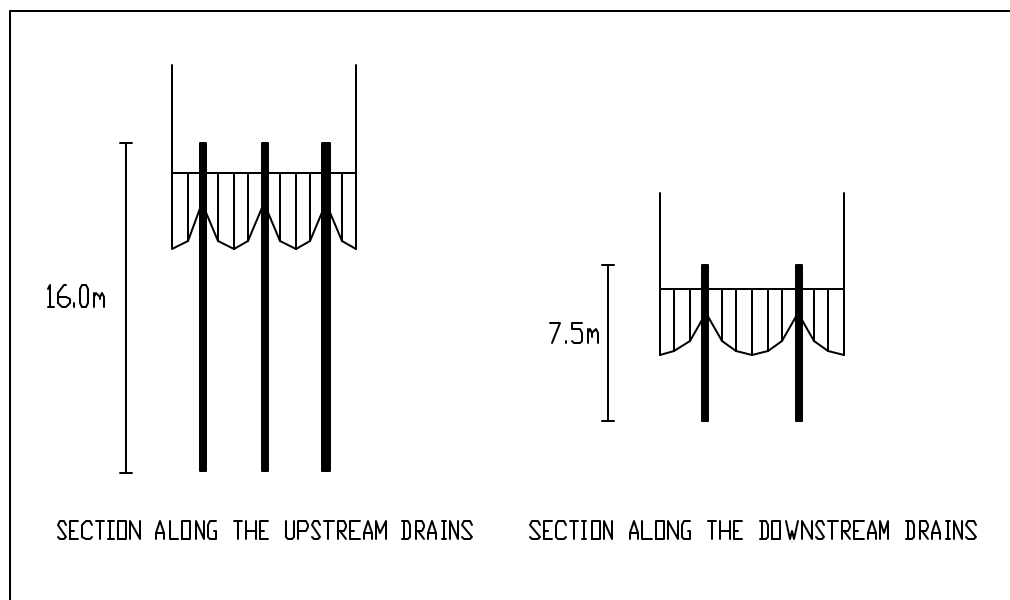


Table 6 – Flow in a typical drain of the upstream drainage gallery

Elevation (m)	Reynolds number	Flow regime	Gradient ($\times 10^{-4}$)	Velocity (m/s)	Discharge (l/min)
127.0 a 128.0	2343.0	Turbulent	0.5340	0.03105	8.496
126.0 a 127.0	1398.0	Laminar	0.1122	0.01853	5.070
125.0 a 126.0	306.9	Laminar	0.0246	0.00407	1.113
123.5 a 125.0	203.6	Laminar	0.0163	0.00270	0.739
122.5 a 123.5	135.8	Laminar	0.0109	0.00180	0.492
120.2 a 122.5	65.2	Laminar	0.0053	0.00086	0.236
119.2 a 120.2	60.6	Laminar	0.0049	0.00080	0.220
117.0 a 119.2	42.3	Laminar	0.0034	0.00056	0.153
114.4 a 117.0	32.9	Laminar	0.0025	0.00044	0.119

- 2 - Casagrande, A., "Control of seepage through foundations and abutments of dams", First Rankine lecture, 1961, in "Milestones in soil mechanics", London, Institution of Civil Engineers, 1975, p.1-21.
- 3 - Serafim, J. L., Del Campo, A., "Interstitial pressure on rock foundations of dams", Journal ASCE, New York, Vol. 91, SM5, p. 65-85, Sept. 1965.
- 4 - Muskat, M., "The flow of homogeneous fluids through porous media", Ann Arbor, J.M. Edwards, 1946, 763p
- 5 - Schneebeli, G., "Hydraulique souterraine", Paris, Eyrolles, 1966, 362p.
- 6 - Neves, E.T., "Course on hydraulics", 2nd edition, Porto Alegre, Editora Globo, 1970, 577p. (in Portuguese)
- 7 - Hubbert, M.K., "The Theory of Ground-Water Motion", J. Geol., Vol. 48, No. 8, Part 1, 1940, p.785-944.
- 8 - Da Silva JF. "A numerical model for three-dimensional analysis of seepage through the foundations of concrete dams supported by permeable continuous rocks". Thesis presented as partial fulfillment for a Doctor of Sciences degree in Rock Mechanics. Federal University of Minas Gerais, Brazil, 2002. (in Portuguese).
- 9 - Engevix – Estudos e Projetos de Engenharia – UHE Balsas Mineiro Report IIE-RT-002 (1984).
- 10 - de Quadros, E.F., Correa Filho, D., de Azevedo, A.A. "Hydraulic three-dimensional tests - comparison of concepts and results with single packer tests", Tunnel and Underground Structures, Zhao, Shirlaw & Krishnan (eds) Balkema, pp 603 to 608, Singapore, Nov, 2000.

Influence of the geometry of the drainage system and of the foundation anisotropy on the uplift pressures under concrete dams

da Silva, J. F.

Cmec – Consulting Geotechnical Engineers - Belo Horizonte - MG, Brazil - cmec@cmec.com.br

Abstract: The distribution of pressures on the foundation of concrete gravity dams, supported on continuous permeable rocks, is a function of the drainage system, comprised of galleries and drains, and of the foundation anisotropy. The influence on the uplift pressures of the number and position of the drainage galleries, of the diameter, spacing, length, roughness and inclination of drains, is investigated for a dam on homogeneous and isotropic material. The analyses were performed using a nonlinear tri-dimensional finite element model. It was concluded that the drain length causes the greatest reductions in the uplift pressures, followed by its spacing and diameter. Tilting the line of drains offers no advantages except when using two lines of drains. The roughness of the drains normally used in concrete gravity dams causes little impact on the uplift pressures. Additional drainage galleries, adequately positioned, lead to reductions in the uplift pressures. The anisotropy of the foundation materials has great influence on the uplift pressures.

Resumo: A distribuição de pressões nas fundações de barragens de concreto gravidade, apoiadas em rochas contínuas permeáveis, é função do sistema de drenagem, composto por galerias e drenos, e da anisotropia dos materiais de fundação. A influência no valor das subpressões do número e posição das galerias de drenagem, do diâmetro, espaçamento, comprimento, rugosidade e inclinação dos drenos, é investigada para uma barragem apoiada em material homogêneo e isotrópico. As análises foram conduzidas através de um modelo numérico tridimensional não linear desenvolvido pelo método dos elementos finitos. Verificou-se que o comprimento dos drenos é o fator que mais influi na redução das subpressões, seguido pelo espaçamento e pelo diâmetro. A inclinação da linha de drenos não oferece vantagens, exceto quando se utilizam duas linhas de drenos. A rugosidade dos drenos comumente usados em barragens de concreto gravidade causa pequenas alterações nas subpressões. A introdução de galerias de drenagem adicionais causa redução das subpressões. A anisotropia dos materiais de fundação exerce grande influência nas subpressões.

1. INTRODUCTION

One of the most important tasks of the geotechnical design of concrete gravity dams is to establish its stability against sliding. Figure 1 depicts the system of forces for a typical concrete dam. The correlation between these forces, to maintain equilibrium, is given by the expression:

$$F_s = \frac{(P - U) \cdot \text{tg}\Phi + cA}{H_m - H_j} \quad (1)$$

where F_s is the factor of safety against sliding, P is the weight of the structure (kN), H_m is the force due to the upstream reservoir (kN), H_j is the force due to the downstream reservoir (kN), U is the force caused by the uplift pressures at the base (kN), Φ is the friction angle at the base ($^\circ$), c is the cohesion (kPa) and A is the area of the base of the structure (m^2).

The cohesion and the friction angle are properties

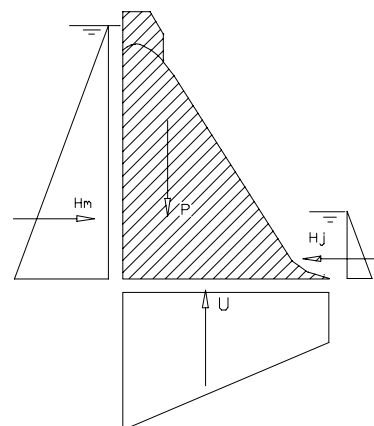


Figure 1 - Forces acting on a typical concrete dam

of the foundation materials. The other elements in expression (1) are determined by hydraulics with the exception of the uplift force which depends on the permeabilities of the foundation materials and on the geometry of the drainage system.

Therefore, the only elements in expression (1) that can be modified by the geotechnical designer are the weight of the structure (P) and the uplift force (U).

Expression (1) shows that the factor of safety increases with increments in the weight of the structure, reductions of the uplift pressures, or both. Consequently, for a given factor of safety, a reduction of the uplift pressures would allow for a reduction in concrete volumes with reflections on the dam's cost and construction time.

Therefore, as the uplift pressures have a strong influence both on the stability and on the cost and construction time of the structure, its control is probably the most important aspect of the geotechnical design of concrete dams.

2. EVALUATION OF UPLIFT PRESSURES

The uplift pressures on concrete gravity dams have been generally estimated through design criteria. The most popular is the criterion proposed by the USBR (Davis, 1969) and indicated in Figure 2.

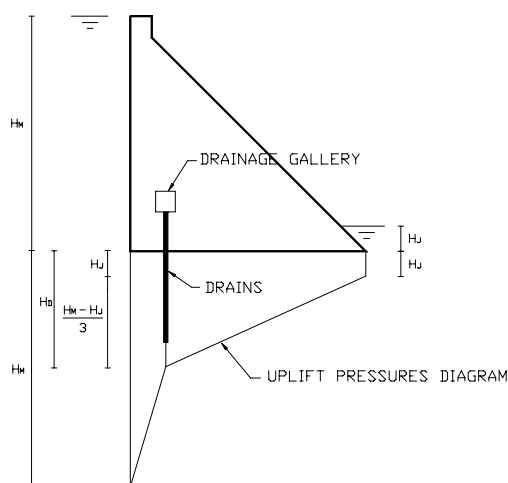


Figure 2 – Design criterion - USBR

The use of the USBR design criterion leads generally to the design of conservative structures, but it could also lead to the design of dams with inadequate safety factors as shown in Figure 3.

In a previous publication (da Silva and da Gama, 2003), it was postulated that the most adequate form to estimate the uplift pressures on concrete gravity dams foundations was by means of flow analyses.

These analyses are tri-dimensional and nonlinear in nature due to the presence of drains. To perform the analyses, a tri-dimensional nonlinear numerical model named DW3D was developed through the finite element method and its details are presented elsewhere (da Silva and da Gama, 2003). Therefore, only its fundamentals are indicated here.

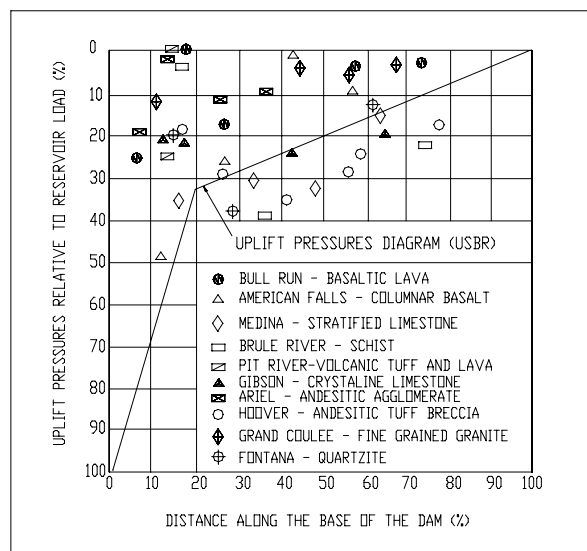


Figure 3 - Uplift pressures in the dam/foundations contact (Apud Serafim and Del Campo, 1965)

2.1 – Fundamentals of model DW3D

The permanent flow through continuous permeable rocks, saturated and incompressible, is generally represented by Darcy's law. In three dimensions Darcy's law is given by the following expressions:

$$V_x = k_x i_x; \quad V_y = k_y i_y \quad e \quad V_z = k_z i_z \quad (2)$$

where V = velocity (m/s); k = coefficient of permeability (m/s); and i = hydraulic gradient.

Furthermore, the expression which allows for the representation of linear flows (function of the first power of the hydraulic gradient) in drains, is Darcy's law for smooth pipes:

$$V_{\text{drain}} = \frac{g D^2}{32\nu} i \quad \text{or} \quad V_{\text{drain}} = "K_{\text{drain}}" i \quad (3)$$

Where V_{drain} = velocity in the drain (m/s); g = acceleration of gravity (m/s^2); D = drain diameter (m); ν = kinematic coefficient of viscosity (m^2/s).

The parameter " K_{drain} " = "coefficient of permeability" for the smooth pipe, is "equivalent" to the coefficient "k" of expression (2), and correspond to:

$$K_{\text{drain}} = \frac{g D^2}{32\nu} \quad (4)$$

The kinematic coefficient of viscosity (ν), is given by Poiseuille's expression:

$$\nu = \frac{1,78 \times 10^{-6}}{1 + 0,0337t + 0,000221t^2} \quad (5)$$

where "t" is the water temperature in degrees centigrade.

The expression that allows for the representation of nonlinear flow (function of the square root of the hydraulic gradient) in drains of circular cross section either smooth or rough and under laminar or turbulent flow, is Weissbach's law for pipes which can be expressed by one of the following forms:

$$\frac{h_f}{L} = i = f \frac{V^2}{2gD} \quad \text{or} \quad V = \sqrt{\frac{2gDi}{f}} \quad (6)$$

where h_f = energy losses (m); f = roughness coefficient; L = drain length (m) .

The roughness coefficient "f" for smooth or rough drains, under laminar flow, is given by the expression:

$$f = \frac{64}{N_R} \quad (7)$$

where N_R is Reynolds' number, expressed by the relation:

$$N_R = \frac{VD}{\nu} \quad (8)$$

The roughness coefficient "f" for rough drains, under transition regime or complete turbulence ($N_R > 2100$), is calculated by means of Colebrook's expression (Neves, 1970):

$$\frac{1}{\sqrt{f}} = -2 \log \left(\frac{h_a}{D} + \frac{2,51}{N_R \sqrt{f}} \right) \quad (9)$$

where " h_a " is the height of the projections ("asperities") in the drain walls (m).

When the flow occurs in a hydraulically smooth drain, "f" should be calculated by the expression due to Nikuradse (Neves, 1970):

$$f = 0,0032 + 0,221 (N_R)^{-0,237} \quad (10)$$

The simulation of the tri-dimensional flow in continuous permeable media, by means of the finite element method has been fully discussed elsewhere (Simunek et al, 1995). Therefore the present discussion will be restricted to the effects on flow caused by the presence of drains. To this end a one dimension finite element was developed, as follows:

Figure 4 shows a one dimension finite element, limited by nodal points I e J, representing a drain subject to flow in the principal direction X' . The figure also indicates a global coordinates system XYZ.

It is assumed that the drain is smooth and the flow is laminar. Therefore, the flow in the drain can be represented by expression (3).

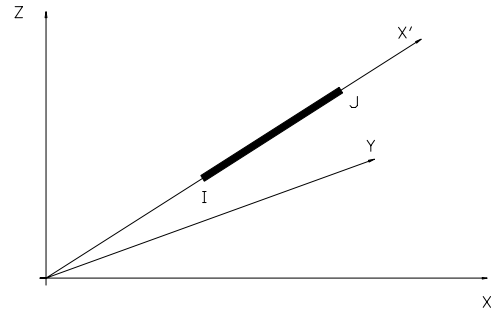


Figure 4 – One dimension drain element

Furthermore, equation (2) can be represented by the following expression (Hubbert, 1940):

$$V_{x'} = -k_{x'} \left(\frac{\partial P}{\partial x'} + \rho g_{x'} \right) \quad (11)$$

where $V_{x'} = V_{\text{drain}}$ = velocity of water in the drain element in the direction X' (m/s); $k_{x'} = k_{\text{drain}}$ = coefficient of permeability of the smooth drain in the direction X' (m/s); P = water pressure at a point inside the element (kPa); ρ = density of water; $g_{x'}$ = component of "g" in direction X' (m/s²).

It has been demonstrated (da Silva and da Gama, 2003) that starting from expression (11) the quantity of flow on the nodal points of the drain element can be calculated by way of the following expression:

$$\begin{Bmatrix} Q_i \\ Q_j \end{Bmatrix} = \begin{bmatrix} \frac{A k_{x'}}{L} & -\frac{A k_{x'}}{L} \\ -\frac{A k_{x'}}{L} & \frac{A k_{x'}}{L} \end{bmatrix} \begin{Bmatrix} P_i \\ P_j \end{Bmatrix} + \begin{Bmatrix} A k_{x'} \rho g \text{ sen } \Theta \\ -A k_{x'} \rho g \text{ sen } \Theta \end{Bmatrix} \quad (12)$$

where Q_i = quantity of flow at nodal point i (m³/s); Q_j = quantity of flow at nodal point j (m³/s); A = area of the drain's cross section (m²); $k_{x'}$ = "equivalent" coefficient of permeability for the drain (m/s); P_i = pressure at nodal point i (kPa); P_j = pressure at nodal point j (kPa); Θ = angle between X e X' ($^\circ$).

In expression (12), the matrix :

$$\begin{bmatrix} \frac{A k_{x'}}{L} & -\frac{A k_{x'}}{L} \\ -\frac{A k_{x'}}{L} & \frac{A k_{x'}}{L} \end{bmatrix} \quad (13)$$

is the stiffness matrix of the drain element.

However, as discussed, the general expression for the flow of water in drains either rough or smooth, under laminar or turbulent regime (expression (6)), is nonlinear. Expression (6) is represented in Figure 5, which indicates the variation of the flow velocity in a drain as a function of the hydraulic gradients. To take into account the non-linearity of expression (6),

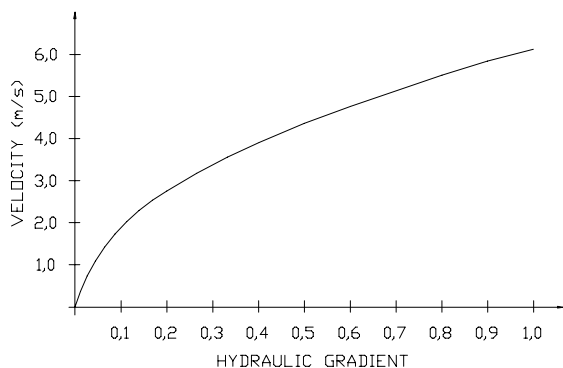


Figure 5 – Nonlinear flow in drains

by means of the finite element method, the following technique was adopted:

In Figure 6, the line with inclination (α_D) represents the linear flow (Darcy) in a "virtual" smooth drain which has, initially, the same diameter as the real drain (Weissbach).

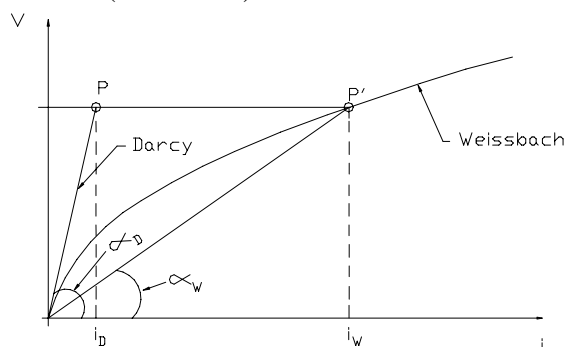


Figure 6 – The virtual drain method (da Silva and da Gama, 2003).

The velocities are also the same for both drains, as indicated by points P and P', but the gradients are different since the "equivalent coefficients of permeability" of the drains are, respectively, equal to:

$$k_{\text{drain}} = \tan(\alpha_D) \quad (\text{virtual}) \quad (14)$$

and

$$k_W = \tan(\alpha_W) \quad (\text{real}) \quad (15)$$

However, according to expression (4), an increase or reduction of the virtual drain diameter causes a correspondent increase or reduction in the value of the equivalent permeability (k_{drain}) of the virtual drain. Therefore, through adequate changes in the value of the virtual drain diameter one can make α_D approach α_W . When convergence is attained between the values of α_D and α_W , the flow in both drains will be the same (although the diameters will be different) and there will be total correspondence of velocities, gradients and flows between the virtual and the real drain. This process is repeated, through successive iterations for each drain element, until convergence is attained:

$$\frac{i_D - i_W}{i_W} \leq \text{tol} \quad (16)$$

where i_D = gradient in the virtual drain; i_W = gradient in the real drain; tol = admitted tolerance

An assessment of accuracy of the DW3D model, by comparison of calculated and observed values of pressures in the foundations of a concrete dam in operation in northern Brazil, has been presented elsewhere (da Silva and da Gama, 2003).

3. INFLUENCE OF DRAINAGE GEOMETRY

As the foundation drainage systems of concrete dams are comprised of drainage galleries and drains, the following aspects of their geometry, which affect the values of the uplift pressures, have been investigated:

- drain length
- drain diameter
- drain spacing
- drain inclination
- drain roughness
- number and position of drainage galleries

3.1. Dam model used for the analyses

In order to perform the flow analyses the concrete dam indicated in Figure 7 was adopted. The dam sits on permeable continuous rock.

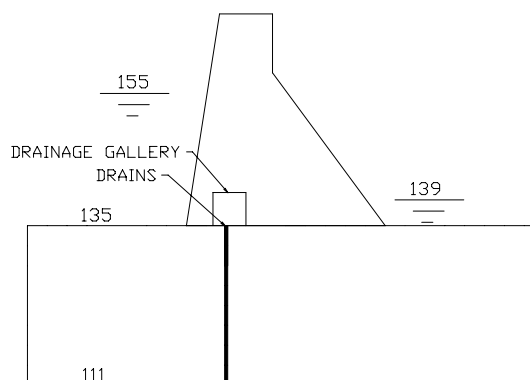


Figure 7 – Dam model used in the analyses

The following basic data were used:

- drain diameter = 0.0762m = 3"
- drain spacing = 6m
- drain length = 20m
- height of roughness in drain walls = 2mm
- water temperature = 20°C

The foundation rock properties related to flow are indicated in Table 1.

System $x'y'z'$ corresponds to the principal directions of the permeabilities.

Parameter	Value
$k_{x'} = k_{y'} = k_{z'}$	10^{-5} m/s
Angle (x',x)	0^0
Angle (y',y)	0^0
Angle (z',z)	0^0
Angle (x',y)	90^0
Angle (y',x)	90^0
Angle (x',z)	90^0
Angle (z',x)	90^0
Angle (y',z)	90^0
Angle (z',y)	90^0

Table 1 – Elements of the permeability tensor

The system xyz has a horizontal "x" axis, directed upstream to downstream. Axis "y", also horizontal, is directed from the right flank to the left flank. Axis "z" is vertical, directed from the bottom to the top of the dam.

Figure 8 indicates a section upstream-downstream passing through one of the drains of the finite element mesh. Figure 9 shows a flank to flank section passing through the line of drains.

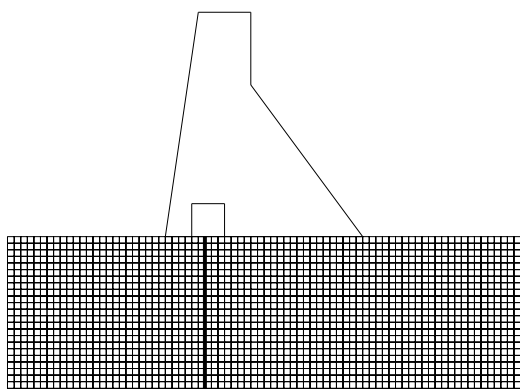


Figure 8 – Finite elements mesh - Section upstream downstream passing through one of the drains

3.2. Influence of drain length

Figure 10 shows a plot of the variation of the uplift forces at the base of the dam with the drains length. As indicated in the figure, the drain length has a large influence on the values of the uplift pressures up to approximately half the value of the upstream reservoir depth. From this point onwards the influence of the drains length decreases up to a value equal to the reservoir depth. Afterwards, its influence is very small.

3.3. Influence of drain spacing

Figure 11 shows the variation of the uplift forces as a function of drains spacing. The uplift force variation with drain spacing is practically linear.

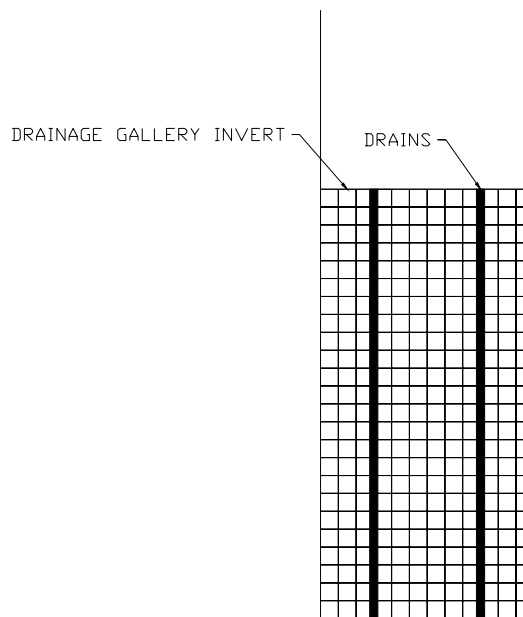


Figure 9 – Finite element mesh - Flank to flank section passing through the line of drains

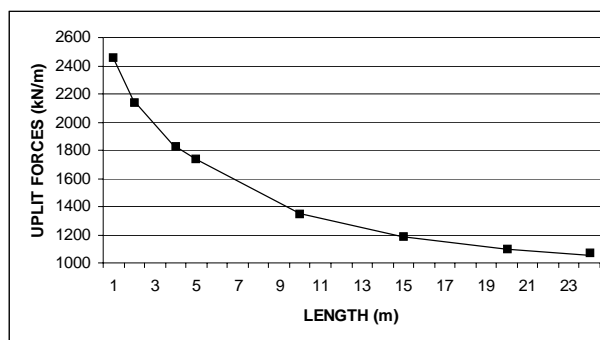


Figure 10 – Uplift forces versus drain length

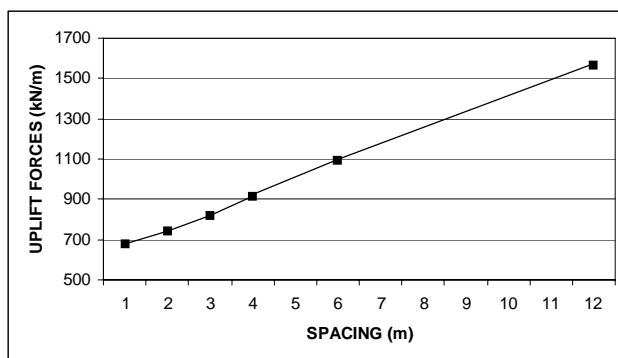


Figure 11 – Uplift forces versus drain spacing

Although the influence of the spacing is proportionally smaller than that of the drain length there will always be reductions of pressures following reductions in spacing.

3.4. Influence of drain diameter

Figure 12 indicates a plot that shows the variation of the uplift forces as a function of the drain diameter and also as a function of the permeability of the foundation rock.

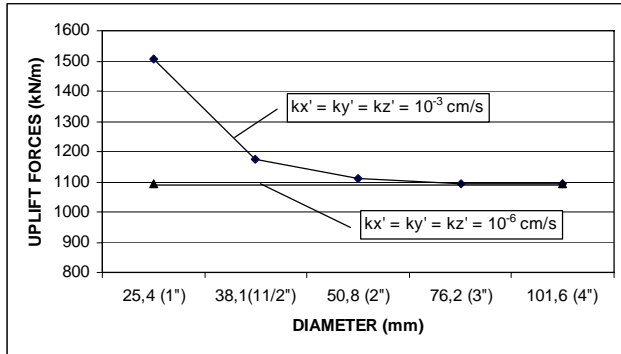


Figure 12 – Uplift forces versus drain diameter and rock permeability

It can be seen from Figure 12 that for the higher permeability rock there is an influence of the drain diameter on the uplift forces up to a value of 50.8mm (2"). From this point onwards the influence is small. The influence of the drain diameter however is negligible when the foundation rock has low permeability and, consequently, both the velocity and flow quantities in the drains are also low.

Figure 13 shows in one plot the variation of the uplift forces at the base of the dam as a function of drain length, diameter and spacing.

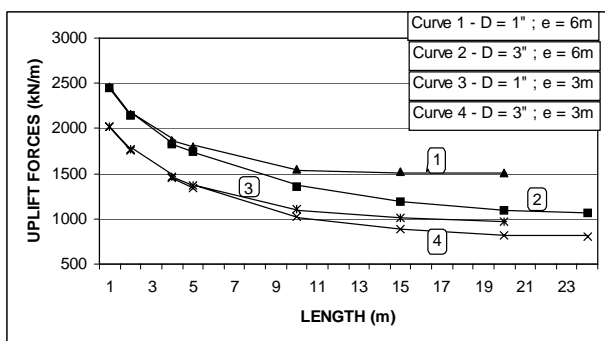


Figure 13 – Uplift forces versus drain length, diameter and spacing

Figure 13 allows comparison of the three main geometrical characteristics of the drains. The following observations can be made from the figure:

- The size of the drains' diameter (D) is a function of their spacing (e). The larger the spacing the larger should be the diameter. For smaller spacing the diameters could also be smaller.

- The drain diameter is a function of its length. Longer drains require larger diameters. Shorter drains could have smaller diameters.

3.5. Influence of drain inclination

Five inclinations of the line of drains were investigated. The drains were tilted anti-clockwise in relation to the point of intersection between the line of drains and the base of the drainage gallery: lines making 25° and 45° with the horizontal (tilting upstream), a vertical line and lines making 135° and 155° with the horizontal (tilting downstream). Figure 14 shows a plot with the variation of the uplift forces at the base of the dam as a function of the drains inclination. An inspection of Figure 14 indicates that inclining the drains either upstream or downstream will increase the uplift pressures. The explanation can be found in Figure 15 that shows the uplift pressures diagrams at the base of the dam for three of the situations investigated.

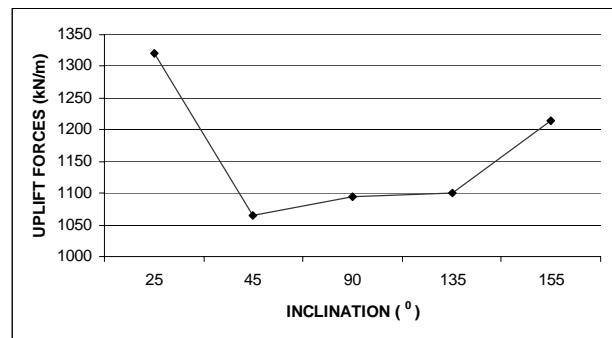


Figure 14 – Uplift forces versus drain inclination

It can be observed that by inclining the drains upstream the portion of the uplift pressure diagram situated between the upstream toe of the dam and the drainage gallery is reduced, but the portion of the diagram situated between the drainage gallery and the downstream toe is increased. The contrary occurs when the drains are inclined downstream.

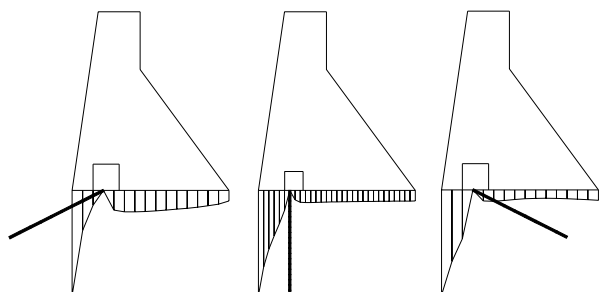


Figure 15 – Uplift pressures diagrams as a function of the drain inclination

However, the use of two lines of drains, one tilting upstream and the other tilting downstream would combine the reductions of the uplift pressures dia-

grams caused by each line of drains. This can be confirmed by inspection of Figure 16, which shows the uplift pressure diagram for this situation.

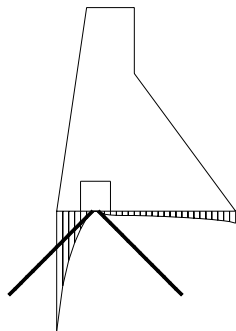


Figure 16 – Uplift pressure diagram for two lines of drains tilting 45°

The uplift reduction caused by the two lines of drains is repeated in Figure 17, for comparison with the uplift values for one single line.

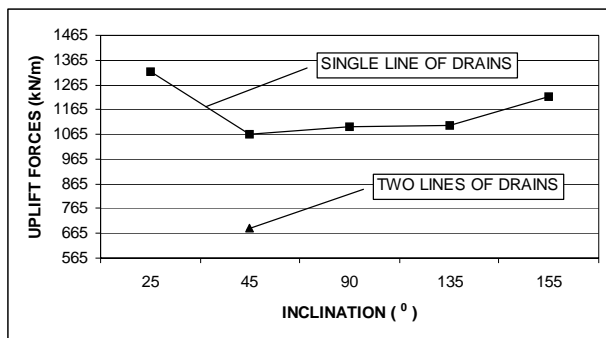


Figure 17 – Uplift forces versus number of drain lines

3.6. Influence of drain roughness

Six different dimensions of drain roughness (wall projections) were investigated: 0mm (smooth drain), 1mm, 2mm, 4mm, 8mm and 10mm.

Figure 18 shows a plot with the variations of uplift forces at the base of the dam as a function of the drain wall projections height.

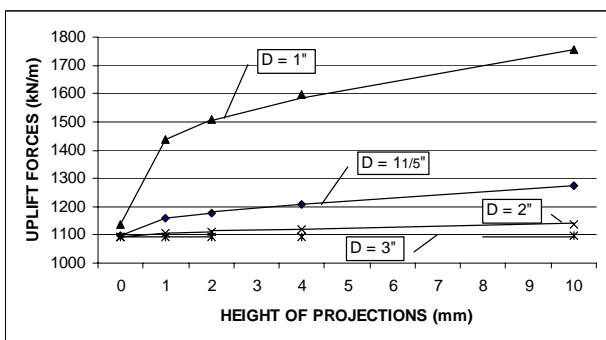


Figure 18 – Uplift forces versus drain roughness

It can be noted that roughness has an influence only for small diameter drains. For the larger diameters usually used in concrete dams, the influence of drain roughness is small. It is interesting to observe that in the case of smooth drains the uplift force will be the same regardless of the drains diameter, confirming previous conclusions (Casagrande, 1961).

3.7. Influence of the number and position of the drainage galleries

The introduction of an additional gallery, in two different positions, shown in Figure 19, was investigated. Figure 20 shows the variation of the uplift forces as a function of the number and position of the drainage galleries and reveals that the introduction of new galleries, together with additional lines of drains, causes reductions in the uplift forces. In addition, the adequate positioning of the galleries allows for further reductions of the uplift pressures.

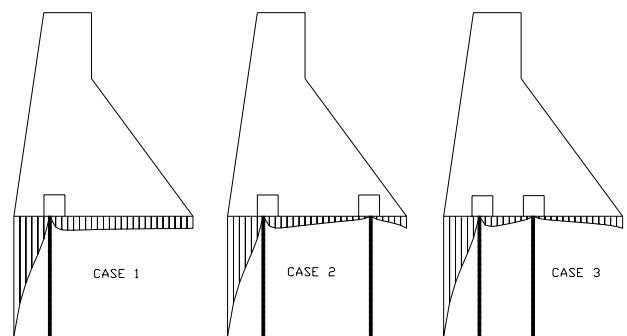


Figure 19 – Number and positions of drainage galleries

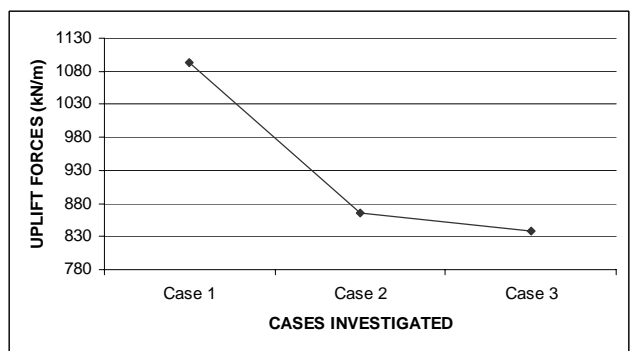


Figure 20 – Uplift forces as a function of the number and position of the drainage galleries

4. INFLUENCE OF ANISOTROPY

To investigate the influence of the foundations anisotropy on the uplift values, three extreme conditions were analyzed, as shown in figures 21, 22 and 23, where the dashed lines indicate the direction of the higher permeabilities.

In the first condition, indicated schematically in Figure 21, it was assumed that the foundation is

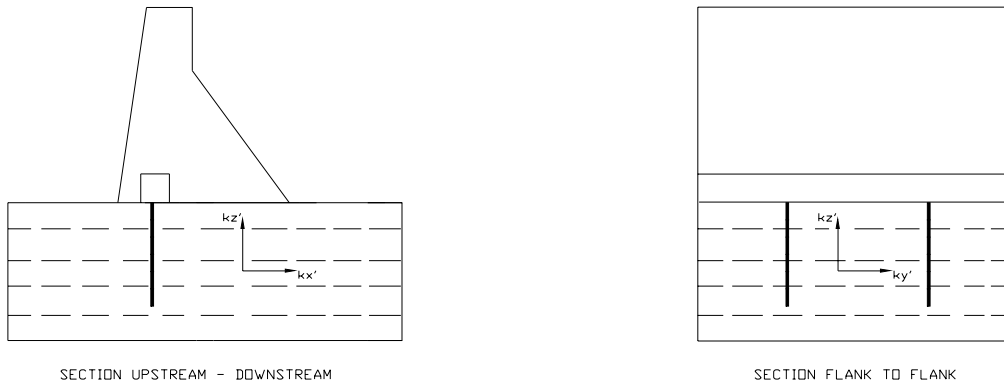


FIGURE 21 - CONDITION 1 - FOUNDATIONS WITH PERMEABILITIES $k_{x'} = k_{y'} > k_{z'}$

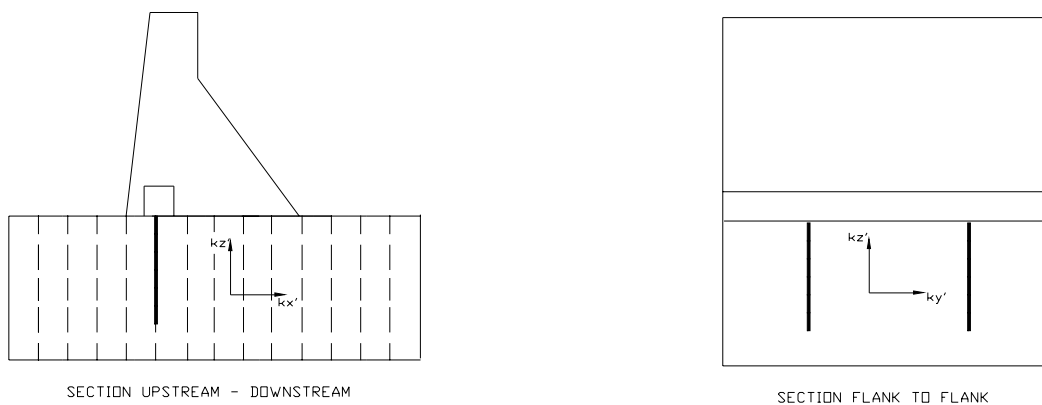


FIGURE 22 - CONDITION 2 - FOUNDATIONS WITH PERMEABILITIES $k_{y'} = k_{z'} > k_{x'}$

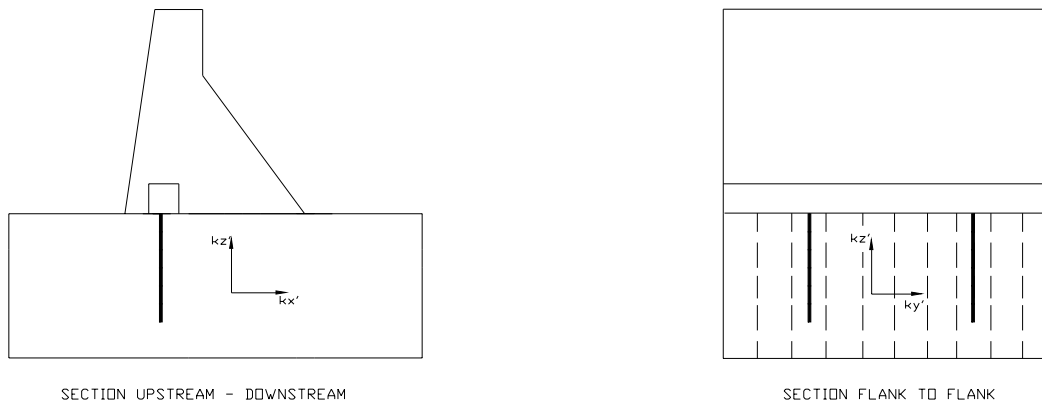


FIGURE 23 - CONDITION 3 - FOUNDATIONS WITH PERMEABILITIES $k_{x'} = k_{z'} > k_{y'}$

formed by materials where $k_{x'} = k_{y'} > k_{z'}$.

In the second condition, indicated in Figure 22, it was assumed that the foundation is formed by materials where $k_{y'} = k_{z'} > k_{x'}$.

In the third condition, indicated schematically in Figure 23, it was assumed that the foundation is formed by materials where $k_{x'} = k_{z'} > k_{y'}$.

4.1. Analysis of the first condition of anisotropy

Figure 24 shows a plot with the variation of the uplift pressures at the base of the dam for the first condition of anisotropy.

It can be seen that changes in uplift pressure at the dam base, due to the increase in anisotropy, are not significant for the condition where the foundation material permeabilities are $k_{x'} = k_{y'} > k_{z'}$.

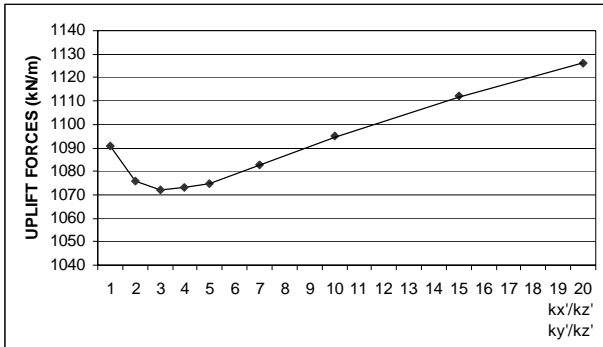


Figure 24 – Uplift forces at the dam base for the condition of $k_{x'} = k_{y'} > k_{z'}$

4.2. Analysis of the second condition of anisotropy

Figure 25 shows a plot with the variation of the uplift forces at the dam base caused by the second condition of anisotropy.

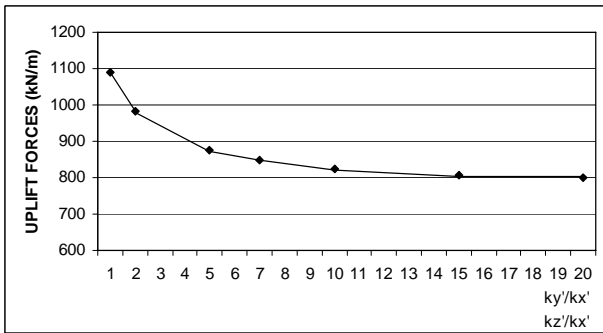


Figure 25 – Uplift forces at the dam base for the condition of $k_{y'} = k_{z'} > k_{x'}$

It can be seen from Figure 25 that the reductions in values of the uplift pressure at the dam base, due to the increase in anisotropy, are significant for the condition where the foundation material permeabilities are $k_{y'} = k_{z'} > k_{x'}$.

4.3. Analysis of the third condition of anisotropy

Figure 26 indicates a plot with the changes in the uplift forces at the dam base for the third condition of anisotropy.

Figure 26 shows that the increments on the uplift forces at the dam base are significant for the condition $k_{x'} = k_{z'} > k_{y'}$.

4.4. Comparison of the cases under study

Figure 27 indicates the values of the uplift pressures under the dam for the conditions of anisotropy shown in Table 2. As observed in Figure 27, anisotropy exerts a strong influence on values of the uplift pressure.

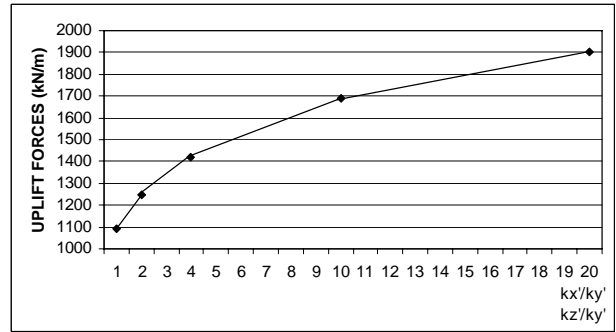


Figure 26 – Uplift forces at the dam base for the condition of $k_{x'} = k_{z'} > k_{y'}$

CASES	PERMEABILITIES
Case 1	$k_{x'} = k_{y'} = k_{z'}$
Case 2	$k_{x'}=20k_{z'}; k_{y'}=20k_{z}'; k_{z'}$
Case 3	$k_{x}'; k_{y'}=20k_{x}'; k_{z'}= 20k_{x}'$
Case 4	$k_{x'}=20k_{y}'; k_{y}'; k_{z'}= 20k_{y}'$

Table 2 – Cases analyzed

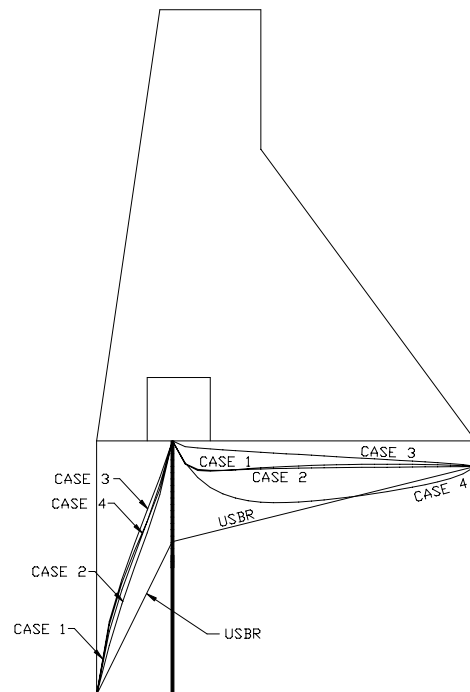


Figure 27 – Uplift pressures diagrams for the conditions of anisotropy described in Table 1

Therefore, the knowledge of the permeability tensors for all materials comprising the foundations is of great importance.

The values of the coefficients of permeability and their corresponding directions are normally obtained by means of special field tests (de Quadros, 1992).

It is also observed in Figure 27 that most of the uplift pressure diagrams for the cases studied (Cases 1 to 3), are situated within the USBR diagram, with the single exception of Case 4. This shows that depending on the particular condition of the foundation anisotropy, the uplift pressures could exceed the values of the USBR diagram.

Observing the plot indicated in Figure 3, it can be noted that the pressure diagrams vary substantially when compared to the USBR diagram. In view of the results of the analyses it is suggested that the reasons for that variation, at least for some of the dams, could be the foundation anisotropy.

4. CONCLUSIONS

Of the three main geometrical properties of the drains, length influences the reduction of the uplift pressures the most, followed by spacing and diameter, in that order. There are however some practical limitations to the drains' length. It has been found that a considerable reduction in the uplift pressures occurs if the drain length is increased up to half the value of the upstream reservoir depth. From this point onwards increases in the drain length will cause proportionally smaller reductions in the uplift pressures until it reaches a length equal to the full reservoir depth. After this point the reductions on the uplift pressures are marginal. The uplift pressures vary linearly with the spacing between drains meaning that there will always be a reduction of the uplift forces with a reduction of drain spacing. The drain diameter only exerts influence in the reduction of the uplift forces if the permeability of the foundation rock is high and the diameters are smaller than 50.8mm (2"). There is a correlation between these three geometrical properties of the drains. Larger spacing requires larger diameters. A reduction in drain spacing will allow for drains of smaller diameter. Longer drains also require larger diameters and shorter drains would allow for the use of smaller diameters. Inclining a single line of drains, either upstream or downstream will increase the uplift pressures. The use of two lines of drains in the same drainage gallery, one line inclined upstream and the other inclined downstream will cause a reduction on the uplift forces. The fourth geometrical property of the drains, its roughness, has influence in the uplift forces only for drains of small diameter. For larger diameters (2" or more), normally used in concrete dams construction, the influence of roughness is very small. The use of additional drainage galleries and lines of drains will always cause reductions in the uplift pressures. An adequate positioning of the

galleries could lead to further reductions. Anisotropy exerts great influence on the values of the uplift pressures and therefore it is very important to determine the permeability tensors for the foundation materials.

5. BIBLIOGRAPHY

- 1 - Casagrande, A., "Control of seepage through foundations and abutments of dams", First Rankine lecture, 1961, in "Milestones in soil mechanics", London, Institution of Civil Engineers, 1975, p.1-21.
- 2 - da Silva, J.F., da Gama, E.M. "A Three-dimensional Model for Seepage Analysis of Concrete Dams Foundations", 4th International Workshop, Applications of Computational Mechanics in Geotechnical Engineering, p.337-357, Ouro Preto - Brazil – 2003.
- 3- de Quadros, E. F., "The Directional Hydraulic Conductivity of Rock Masses", Doctor of Sciences Thesis (in Portuguese), Volume 1, 490p, University of Sao Paulo, Brazil, 1992.
- 4 - Davis, C. V., "Concrete dams, basic principles of design", In: "Handbook of applied hydraulics", Edited by Davis, C.V. e Sorensen, K.E., Third Edition, McGraw-Hill, 1969, Section 9, p.9-1 to 9-34.
- 5 - Hubbert, M.K., "The Theory of Ground-Water Motion", J. Geol., Vol. 48, No. 8, Part 1, 1940, p.785-944.
- 6 - Neves, E.T., "Course on hydraulics", 2nd edition, Porto Alegre, Editora Globo, 1970, 577p. (in Portuguese)
- 7 - Serafim, J. L., Del Campo, A., "Interstitial pressure on rock foundations of dams", Journal ASCE, New York, Vol. 91, SM5, p. 65-85, Sept. 1965.
- 8 - Simunek, J., Huang, K., van Genuchten, M. Th., "The Swms3d code for simulating flow and solute transport in three-dimensional variably-saturated media", Riverside, California, Research report no. 139, U.S. Salinity Laboratory, July, 1995,155p.

Optimization of concrete gravity dams foundation drainage systems

J.F. Da Silva

CMEC - Consulting Engineers, Belo Horizonte, Minas Gerais, Brazil

ABSTRACT: Numerical three-dimensional nonlinear flow analysis is a very efficient instrument for the optimization of the subsurface drainage systems of concrete gravity dams. Post-mortem optimization analyses of the intake and powerhouse structures of Isamu Ikeda dam indicated that the drains' lengths, spacings and diameters used in design were very close to optimum. The analyses have also indicated that the uplift force effectively acting at the structures' base is of the order of 25% of that obtained using the USBR design criterion. The introduction of an additional drainage gallery together with two lines of inclined drains, in all galleries, would have caused an additional reduction in the uplift force to a value near 10% of that indicated by the USBR criterion suggesting that if the present methodology had been available at the design stage of Isamu Ikeda dam it would have been possible to reduce the concrete structures' weight by nearly 40%.

1 INTRODUCTION

One of the most relevant activities of the geotechnical design of concrete gravity dams is the determination of its stability to sliding. Figure 1 shows the system of forces that acts on a typical dam.

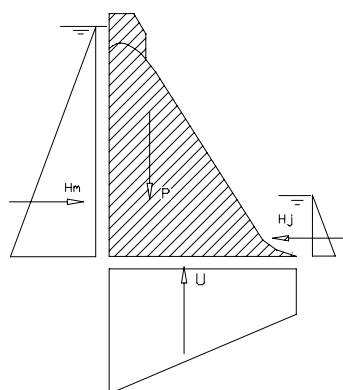


Figure 1 - Forces acting on a concrete gravity dam

The correlation between these forces, to maintain equilibrium, is given by the expression:

$$F_s = \frac{(P - U) \cdot \text{tg}\Phi + cA}{H_m - H_j} \quad (1)$$

where F_s is the shear safety factor, P is the total weight of the structure (kN), H_m is the thrust of the upstream reservoir (kN), H_j is the thrust of the down-

stream reservoir (kN), U is the uplift force caused by the water pressure acting at the dam's base, Φ is the friction coefficient ($^\circ$), c is the cohesion (kPa) and A the area of the base of the structure (m^2).

Expression (1) shows that the safety factor increases with increments in the weight of the structure or with reductions to the uplift force. As the structure's weight can be modified, through changes to its geometry, a reduction of the uplift force would allow for a reduction of the concrete volume and therefore of the structures' cost and construction time. Since the uplift force has such a strong influence both on stability and cost of the structure, its control is probably the most important aspect of the geotechnical design of concrete dams.

2 DETERMINATION OF THE UPLIFT FORCE

The uplift pressures caused by seepage through the foundations of concrete gravity dams has been generally estimated based on certain design criteria, the criterion proposed by the USBR (Davis, 1969) and indicated in Figure 2 being that most used.

The use of the USBR design criterion leads, in most cases, to the design of conservative structures in terms of safety factors to sliding but, sometimes, it can lead to the design of dams with inadequate safety factor values (Serafim & Del Campo, 1965).

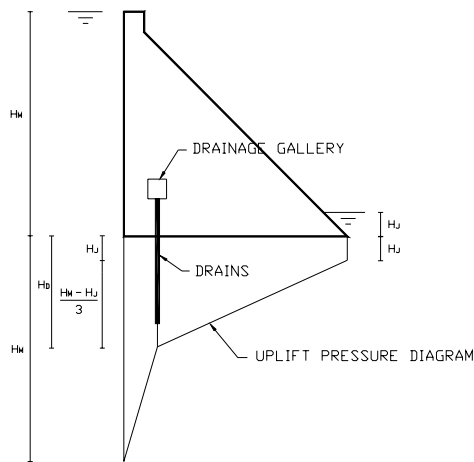


Figure 2 – USBR Design Criterion

In a previous paper (da Silva & da Gama, 2003), it was postulated that the most adequate form of estimating the uplift pressures in the foundation of concrete dams lying on continuous permeable rock would be through adequate seepage analyses capable of incorporating the three-dimensional and nonlinear characteristics imposed on the flow by the presence of the drains drilled from the drainage galleries. A numerical model which includes the above characteristics was developed by means of the finite element method and was denominated DW3D. The model accuracy was then verified comparing the results of the analyses with the instrumentation data of Isamu Ikeda dam, in operation in northern Brazil since 1982, and the agreement between observed and calculated pressure values was very good (da Silva & da Gama, 2003). The results have also shown that the uplift pressure diagram at the base of the structure as determined by the USBR criterion was much larger than that determined by means of the numerical model.

3 DRAINAGE SYSTEM GEOMETRY

In a subsequent paper (da Silva, 2005) the influence of the drainage system geometry on the uplift pressure under concrete gravity dams with drainage galleries and drains was discussed. The geometry of the drains (length, diameter, spacing, roughness and inclination) was investigated together with the number and position of the drainage galleries. It was concluded that the drainage system geometry has a large influence on the values of the uplift pressure.

4 FOUNDATION ANISOTROPY

In that same paper (da Silva, 2005) the influence of the foundation materials anisotropy on the uplift pressure was investigated and the conclusion was that its influence is also very large.

Therefore, the determination of the permeability tensors for the foundation materials, through special field tests (de Quadros, 1992), is a requirement for the realization of adequate flow analyses.

5 OPTIMIZATION OF DRAINAGE SYSTEMS

The optimization of foundation drainage systems of concrete gravity dams consists in determining the number and position of the drainage galleries and the positions, inclinations, lengths, diameters and spacings for the drains in order to reduce the uplift pressure to adequate values.

Reductions to the uplift force (U) will permit the structure's weight (concrete volume) to be also reduced without changes to the safety factor value, as indicated in expression (1).

6 THE ISAMU IKEDA DAM

Figure 3 shows a cross-section through the structures of block number 2, one of the four blocks that comprises the intake and powerhouse complex of Isamu Ikeda dam. This block has been chosen because it contains the piezometers installed in the dam's foundations. More details can be found in da Silva & da Gama (2003).

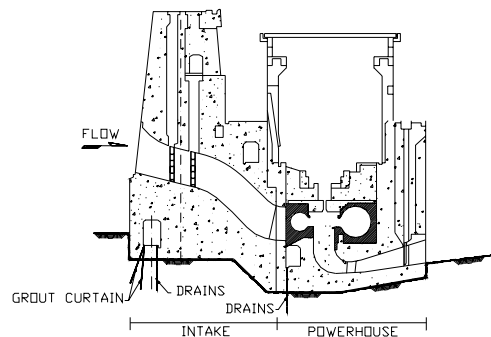


Figure 3 – Typical cross section of block 2 of the intake and powerhouse structures of Isamu Ikeda dam

7 OPTIMIZATION OF ISAMU IKEDA DAM

7.1 Original drainage system geometry

The drainage system built for the structures is indicated, schematically, in Figure 4. The system is comprised of two drainage galleries with one line of vertical drains each. The drains on both galleries have diameters of 76mm(3"). The spacing of the drains in the upstream gallery is 3m and in the downstream gallery is 4.5m. The drains' lengths are 16m and 7.5m respectively.

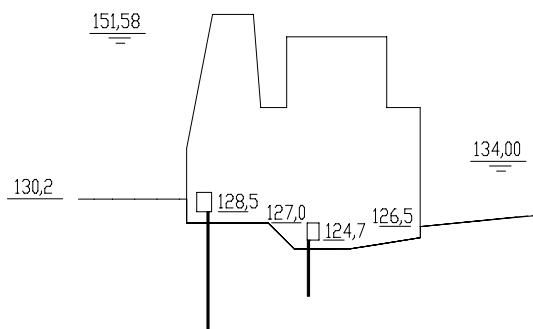


Figure 4 – Original drainage system

7.2 Uplift pressure at the base

A flow analysis, using model DW3D, was performed for the original drainage system and the resulting pressure diagram at the dam's base is shown in Figure 5 together with the USBR diagram. The uplift force (U) resulting from each diagram was 1075.5 kN/m (DW3D) and 4482.0 kN/m (USBR).

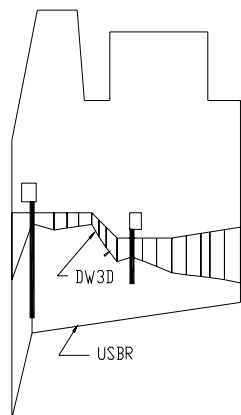


Figure 5 – Uplift Pressure Diagrams at the base of Isamu Ikeda dam (da Silva & da Gama, 2003)

7.3 Reduction of the uplift pressure

As discussed elsewhere (da Silva, 2005), the following actions generally provide reductions to the uplift pressures:

- longer drains
- smaller spacing between drains
- larger diameter drains
- relocation of galleries
- additional galleries
- lines of drains duplicated and inclined

A discussion on the influence of each of these measures to reduce the uplift pressure in the foundations of Isamu Ikeda dam follows.

a) Longer drains

The drains at the upstream gallery were increased in length from their original 16m to 21m and the drains at the downstream gallery from 7.5m to 10m. For this new situation the uplift force (U) at the base is equal to 1071.5 kN/m, indicating a very small reduction. This is in accordance with previous studies, since the drains' original lengths in Isamu Ikeda dam are close to the reservoir's water heads and, therefore, are already optimized in this respect (da Silva, 2005).

b) Smaller spacing

The spacing between drains was then reduced by 50% from 3m to 1.5m for the upstream drains and from 4.5 to 2.25m for the downstream drains. The shortening of the distance between the upstream drains alone led to a reduction of (U) to a value of 1043.8kN/m. The same action applied to the downstream drains reduced (U) to a value of 1039.9kN/m. The shortening of the drains' spacings in both galleries caused a further reduction of (U) to a value of 1008.7kN/m. It can be seen that the reduction of (U), by shortening the drains' distances was small, of the order of 6%, and this is explained by the fact that the original spacings were already adequate (da Silva, 2005).

c) Larger diameter drains

The drains' diameters were increased from 76mm (3") to 100mm (4") resulting in no changes to the uplift pressures, as expected (da Silva, 2005).

d) Relocation of gallery

The downstream gallery was relocated to the position shown in Figure 6. This change reduced (U) to a value of 1015.3 kN/m.

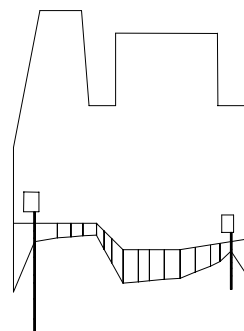


Figure 6 – Uplift pressure diagram with the gallery closer to the downstream face

e) *Additional gallery*

An additional gallery was introduced in the position shown in Figure 7. This measure caused a significant reduction in (U) to a value of 702.8kN/m.

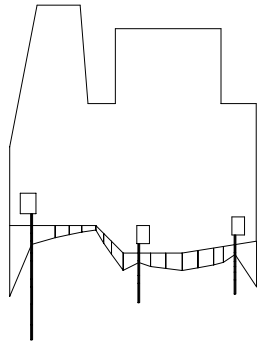


Figure 7 – Uplift pressure diagram for three galleries

f) *Additional drain lines*

The vertical line of drains in the upstream gallery was then replaced by two inclined lines of drains. Figure 8 shows the resultant pressure diagram. The (U) value was equal to 641.7kN/m.

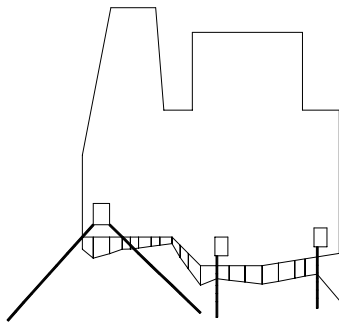


Figure 8 – Uplift pressure diagram for two inclined lines of drains in the upstream drainage gallery

The same action on the intermediate gallery led (U) to a value of 651.0kN/m. This situation is indicated in Figure 9.

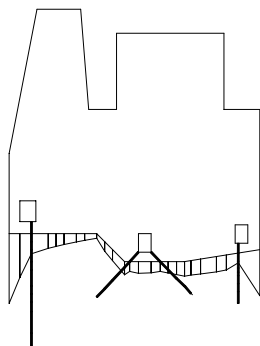


Figure 9 – Uplift pressure diagram for two inclined lines of drains in the intermediate drainage gallery

The introduction of two inclined lines of drains in the downstream gallery, as shown in Figure 10, led (U) to a value of 671.2kN/m.

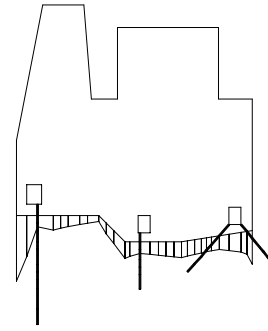


Figure 10 – Uplift pressure diagram with two inclined lines of drains in the downstream drainage gallery

Finally, the introduction of two inclined lines of drains in all galleries, simultaneously, as shown in Figure 11, led (U) to a value of 542.3kN/m.

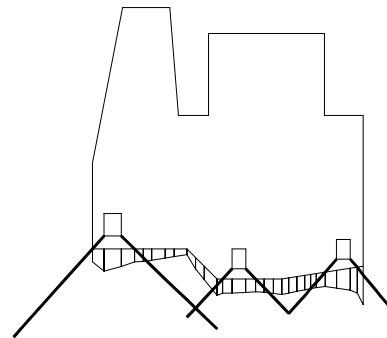


Figure 11 – Uplift pressure diagram for two inclined lines of drains in all galleries

7.4 *Summary of the analyses results*

Table 1 presents a summary of all cases analyzed and the corresponding values of the uplift force U.

From Table 1 it can be observed that the largest reduction in the value of the uplift force, resulting from use of the USBR criterion, occurred by actually taking into account the original geometry of the drainage system in the DW3D flow analysis. This fact alone led to a reduction of 76% in (U) values at the base of the structures, as shown in Figure 12.

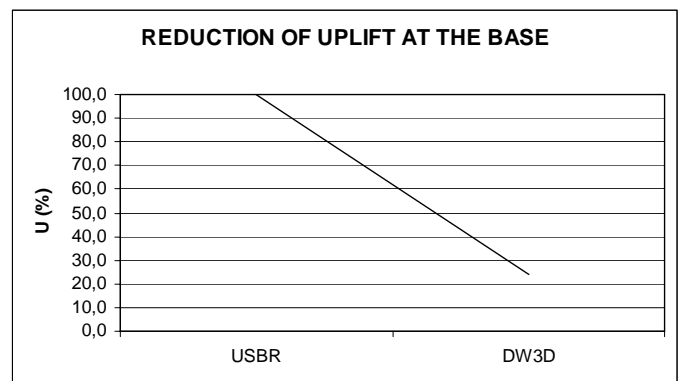


Figure 12 – Reduction of uplift pressure at the base of the structures - Original drainage system

Case	Description	(U) (kN/m)
Case 1	USBR design criterion	4482.0
Case 2	Basic case - Original drainage system	1075,5
Case 3	Longer drains	1071,5
Case 4	Smaller spacing - upstream drains	1043,8
Case 5	Smaller spacing - downstream drains	1039,9
Case 6	Smaller spacing - upstream and downstream drains simultaneously	1008,7
Case 7	Larger drain diameters	1075,5
Case 8	New position for the downstream gallery	1015,3
Case 9	Additional gallery	702,8
Case 10	Additional gallery - Two lines of inclined drains - upstream gallery	641,7
Case 11	Additional gallery - Two lines of inclined drains - central gallery	651,0
Case 12	Additional gallery - Two lines of inclined drains - downstream gallery	671,2
Case 13	Optimized case - Additional gallery - Two lines of inclined drains - all galleries	542,3

Table 1 - Cases analyzed and corresponding values of the uplift force at the base of the structures in relation to the USBR value

The use of longer drains, shorter distances between drains or larger diameter drains caused small reductions in U values. As explained, this is due to the fact that these parameters are already very close to their optimum values.

However, as indicated in Figure 13, the introduction of an additional gallery together with double lines of inclined drains in all galleries caused a further reduction in U of the order of 50% (from 25% to 12%). This means that after the optimization process the final value of U is nearly 12% of that indicated by the USBR criterion.

7.5 Stability analyses

Following the original design, stability analyses were carried out along the horizontal plane (A-A), shown in Figure 14.

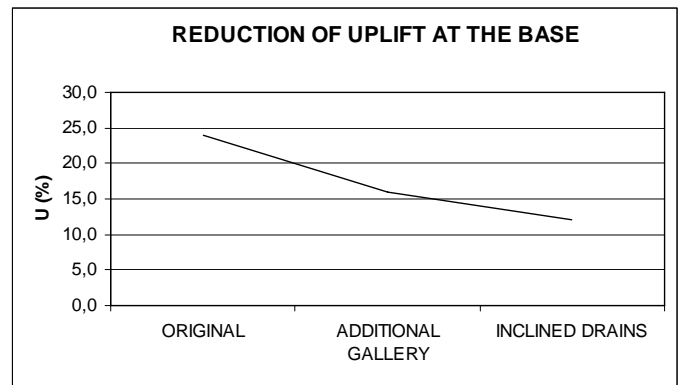


Figure 13 – Reduction of uplift pressure at the base of the structures as a result of the drainage system's optimization

The hatched areas represent blocks of rock and water wedges that have been incorporated into the stability analyses by the designer.

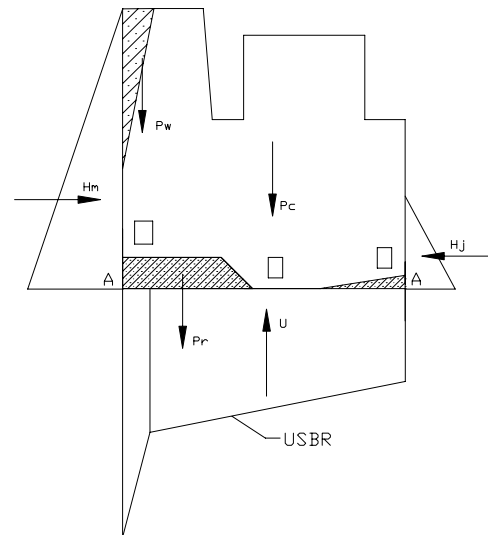


Figure 14 – Sliding stability analysis for the uplift pressure on Plane A-A – Basic Case

From Figure 14 we have:

$$P = P_c + P_r + P_w \quad (2)$$

where P is the total weight of the structures (kN/m), P_c is the concrete weight (kN/m), P_r is the weight of the rock blocks (kN/m) and P_w is the weight of the water wedges (kN/m).

Taking expression (2) into expression (1) we have the following expression to determine the weight of concrete (P_c) for the structures:

$$P_c = \frac{Fs(H_m - H_j) - cA}{tg\phi} + U - P_w - Pr \quad (3)$$

- Design parameters

In all stability analyses the following parameters were assumed constant:

$$P_w = 322 \text{ kN/m}$$

$$P_r = 1414 \text{ kN/m}$$

$$H_m = 4061 \text{ kN/m}$$

$$H_j = 551 \text{ kN/m}$$

$$\Phi = 30^\circ$$

$$c = 0 \text{ kPa}$$

$$FS = 1.5$$

Introducing the values of these parameters in (3), we have:

$$P_c = 7385.25 + U \tag{4}$$

This expression gives the variation of the structures' concrete weight as a function of the uplift force (U), acting along plane (A-A), for a safety factor of 1.5.

Figure 15 depicts expression (4) in graphical form.

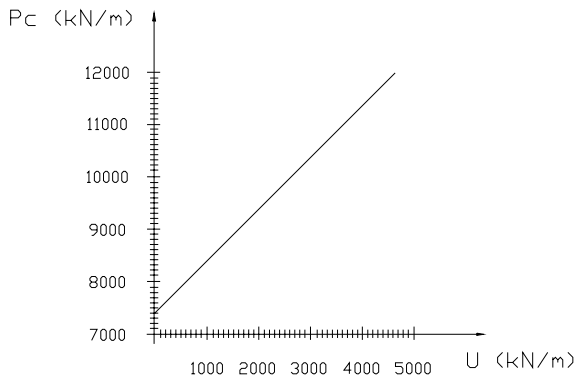


Figure 15 – Variation of the structures' concrete weight as a function of the uplift force on plane A-A

- Cases analyzed

Two cases were analyzed: the basic case and the optimized case, the difference between them being the drainage systems and therefore the values of U on plane (A-A).

- Basic case:

The drainage system, for the basic case, is shown in Figure 4 and corresponds to the original system designed and constructed for the structures of the intake and powerhouse.

In this case the uplift force (U) on plane A-A, indicated in Figure 14, was determined using the USBR criterion and its value was equal to 4397 kN/m.

For this value of (U) Figure 15 indicates that the concrete weight P_c would be equal to 11780 kN/m.

- Optimized case:

The drainage system for the optimized case is indicated in Figure 16.

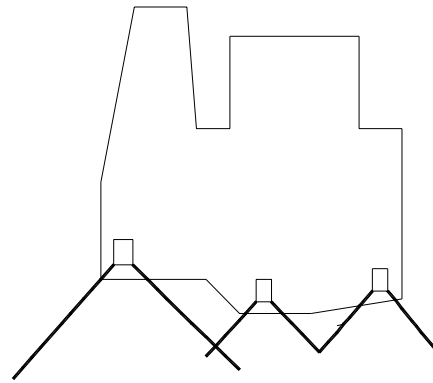


Figure 16 – Optimized drainage system

The diameter of all drains is equal to 76mm(3"). The spacing of the drains in the upstream gallery is 3m and in the intermediate and downstream galleries is 4.5m. The length of the upstream gallery drains is 16m and in the other galleries 7.5m.

In this case, the uplift force on plane A-A, indicated in Figure 17, has been determined by means of the DW3D model and resulted in 973 kN/m. For this value of (U) Figure 15 indicates $P_c = 8356 \text{ kN/m}$.

The results show a difference of 41% in the structures' concrete weight between the basic case and the optimized case.

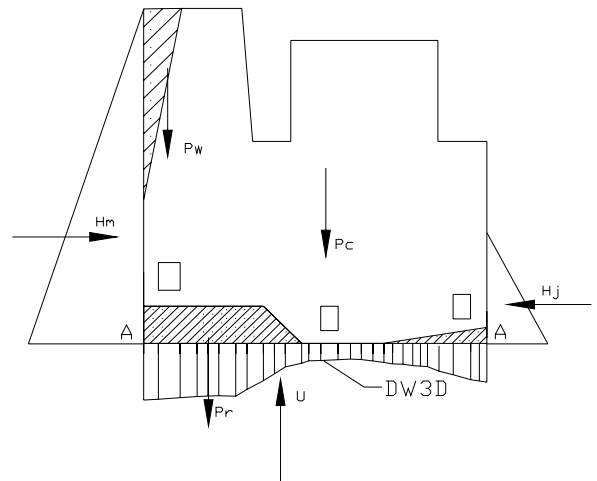


Figure 17 – Sliding stability analysis for the uplift pressure on Plane A-A – Optimized Case

8 CONCLUSIONS

The flow analyses, realized with the intention of optimizing the subsurface drainage system of the structure formed by block 2 of the intake and powerhouse of Isamu Ikeda dam, have shown that the lengths, spacings and diameters originally designed were already very close to their optimum values. The flow analyses performed for the original drainage system geometry have shown that the uplift force value at the dams' base is of the order of 25% of the value estimated through the USBR criterion. This represents a decrease of 75% in the value of (U) as compared to the value used in design. The optimized drainage system consisting of three drainage galleries together with double lines of inclined drains, replacing the single vertical line in each gallery, induced a further 50% reduction in the uplift pressure to a final value near 10% of that indicated by the USBR criterion. This is a reduction of nearly 90% in the value of (U) as compared to the value used in design. A comparison between the sliding stability analyses performed using the USBR uplift pressure diagram and the pressure diagram obtained through DW3D for the optimized drainage system, has shown that if the present approach had been available at the design stage of Isamu Ikeda dam there could have been a reduction of nearly 40% in the structures' concrete weight for a safety factor value of 1.5. It is concluded that flow analyses, along the proposed lines, are a very good instrument for the optimization of subsurface drainage systems of concrete gravity dams and can lead to appreciable reductions in their costs and construction time.

9 REFERENCES

- da Silva, J.F. & da Gama, E.M. 2003. A Three-dimensional model for seepage analysis of concrete dams foundations. *4th International Workshop - Applications of Computational Mechanics in Geotechnical Engineering*. 337-357. Ouro Preto. Brazil.
- da Silva, J.F. 2005. Influence of the geometry of the drainage system and of the foundation anisotropy on the uplift pressures under concrete dams. *Infogeo 2005 - 5th Brazilian Symposium on Applications of Computational Mechanics in Geotechnical Engineering*. 165-174, Belo Horizonte, Brazil.
- de Quadros, E. F. 1992. The directional hydraulic conductivity of rock masses. Doctor of Sciences Thesis. University of Sao Paulo. Volume 1. (In Portuguese).
- Davis, C. V. 1969. Concrete dams, basic principles of design., In Davis, C.V. & Sorensen, K.E (ed), *Handbook of applied hydraulics*. Third Edition: McGraw-Hill, Section 9.

- Serafim, J. L. & Del Campo, A.. 1965. Interstitial pressure on rock foundations of dams. *Journal ASCE*. Vol 91, SM5, 65-85. New York.